




Hyperintense Liver Masses at Hepatobiliary Phase Gadoteric Acid-enhanced MRI: Imaging Appearances and Clinical Importance

Nobuhiro Fujita, MD
 Akihiro Nishie, MD
 Yoshiki Asayama, MD
 Kousei Ishigami, MD
 Yasuhiro Ushijima, MD
 Daisuke Kakihara, MD
 Tomohiro Nakayama, MD
 Koichiro Morita, MD
 Keisuke Ishimatsu, MD
 Hiroshi Honda, MD

Abbreviations: B-HCA = β -catenin-activated HCA, FNH = focal nodular hyperplasia, HBP = hepatobiliary phase, HCA = hepatocellular adenoma, HCC = hepatocellular carcinoma, H-HCA = hepatocyte nuclear factor 1 α -mutated HCA, I-HCA = inflammatory HCA, IPNB = intraductal papillary mucinous neoplasm of the bile duct, LI-RADS = Liver Imaging Reporting and Data System, MRP = multidrug resistance-associated protein, NRH = nodular regenerative hyperplasia, OATP1B3 = organic anion-transporting polypeptide 1B3, U-HCA = unclassified HCA

RadioGraphics 2020; 40:0000-0000

<https://doi.org/10.1148/rg.2020190037>

Content Codes:   

From the Departments of Clinical Radiology (N.F., A.N., K. Ishigami, Y.U., D.K., K.M., K. Ishimatsu, H.H.), Advanced Imaging and Interventional Radiology (Y.A.), and Molecular Imaging and Diagnosis (T.N.), Graduate School of Medical Sciences, Kyushu University, 3-1-1 Maidashi, Higashi-ku, Fukuoka 812-8582, Japan. Presented as an education exhibit at the 2018 RSNA Annual Meeting. Received March 2, 2019; revision requested June 26 and received July 7; accepted July 15. For this journal-based SA-CME activity, the author T.N. has provided disclosures (see end of article); all other authors, the editor, and the reviewers have disclosed no relevant relationships. **Address correspondence to** N.F. (e-mail: n-fujita@radiol.med.kyushu-u.ac.jp).

See discussion on this article by Lalwani (pp 23-26).

©RSNA, 2019

Gadoteric acid, a hepatobiliary-specific contrast medium used for MRI, is becoming increasingly important in the detection and characterization of hepatic mass lesions. This medium is taken up by functioning hepatocytes, and the liver parenchyma is strongly enhanced in the hepatobiliary phase (HBP), during which hepatic mass lesions without functioning hepatocytes commonly show hypointensity. However, some hepatic mass lesions show hyperintensity in the HBP. Focal nodular hyperplasia (FNH) and FNH-like lesions show hyperintensity in the HBP owing to the uptake of gadoteric acid by hyperplastic normal hepatocytes. The tumor cells of some types of hepatocellular adenoma (eg, β -catenin-activated type, inflammatory type) and hepatocellular carcinoma (eg, green hepatoma) can show uptake of gadoteric acid. Retention of gadoteric acid in the extracellular space can cause hyperintensity of fibrotic tumors or hemangiomas during the HBP owing to the extracellular contrast agent characteristics of gadoteric acid. During the HBP, peritumoral retention is observed in some tumors, such as hepatocellular carcinomas, gastrointestinal stromal tumors, and neuroendocrine tumors. Gadoteric acid is excreted into the bile; therefore, biliary tract enhancement can be observed in the cystic components of intraductal papillary neoplasms of the bile duct. Intratumoral bile ducts can be observed in malignant lymphomas. Knowledge of these specific mechanisms, which can cause hyperintensity during the HBP depending on the pathologic or molecular background, is important not only for precise imaging-based diagnoses but also for understanding the pathogenesis of hepatic mass lesions.

©RSNA, 2019 • radiographics.rsna.org

SA-CME LEARNING OBJECTIVES

After completing this journal-based SA-CME activity, participants will be able to:

- List the spectrum of hepatic mass lesions that can show hyperintensity during the HBP of gadoteric acid-enhanced MRI.
- Describe the pathologic and molecular features, clinical significance, and usefulness of the differential diagnoses of hyperintense hepatic masses seen at gadoteric acid-enhanced MRI.
- Discuss the clinical usefulness of gadoteric acid-enhanced MRI for improved image interpretation and patient care.

See rsna.org/learning-center-rg.

TEACHING POINTS

- Hepatic mass lesions can show hyperintensity partially or entirely during the HBP owing to the following mechanisms: (a) uptake by hyperplastic hepatocytes, (b) uptake by tumor cells, (c) retention in extracellular space, (d) peritumoral retention, and (e) biliary enhancement in the tumor.
- B-HCA is the most common HCA subtype that takes up gadoxetic acid. According to previous reports, more than 80% of B-HCA lesions show isointensity or hyperintensity during the HBP.
- Approximately 10%–15% of HCCs are hyperintense during the HBP, and the distinct pathologic and biologic characteristics of hyperintense HCCs have been reported.
- Liver lesions that have expanded extracellular volume, such as fibrosis and necrosis, possibly demonstrate gadoxetic acid retention in the extracellular space during the HBP owing to the properties of gadoxetic acid that are similar to those of conventional extracellular contrast material.
- Histopathologically, peritumoral retention corresponds to peritumoral hyperplasia, which is defined as a rim of hyperplastic hepatocytes surrounding the tumor.

Introduction

Gadoxetic acid (gadolinium ethoxybenzyl diethylenetriamine pentaacetic acid [Eovist or Primovist; Bayer Healthcare, Berlin, Germany]) is a hepatobiliary-specific contrast medium used for MRI (1,2). This agent is becoming increasingly important for detecting and characterizing lesions in patients known or suspected to have hepatic mass lesions (3,4). During the hepatobiliary phase (HBP), hepatic mass lesions without functioning hepatocytes commonly show hypointensity relative to the background liver tissue. Compared with conventional extracellular contrast material-enhanced CT or MRI, gadoxetic acid-enhanced MRI has been proven to have higher sensitivity in the detection of hepatic mass lesions because of this feature (5,6).

However, hepatic mass lesions can show hyperintensity partially or entirely during the HBP owing to the following mechanisms (Table 1): (a) uptake by hyperplastic hepatocytes, (b) uptake by tumor cells, (c) retention in extracellular space, (d) peritumoral retention, and (e) biliary enhancement in the tumor. Understanding these mechanisms as they relate to the HBP findings and pathologic and/or molecular background is useful for image interpretation and understanding the pathogenesis of hepatic mass lesions.

In this article, we review the hepatic mass lesions that can demonstrate hyperintensity during the HBP of gadoxetic acid-enhanced MRI. This review article is especially focused on (a) the spectrum of imaging findings of hepatic mass lesions that may show hyperintensity during the HBP, (b) the pathologic and molecular features that cause hyperintensity during the HBP, (c) the

clinical significance of hyperintensity during the HBP, and (d) the usefulness of the differential diagnoses of hepatic mass lesions.

Kinetic Features of Gadoxetic Acid

Gadoxetic acid has the properties of a conventional nonspecific extracellular contrast agent during the vascular phases after it is administered and thus enables dynamic imaging for evaluation of vascularity. During the HBP, approximately 20 minutes after this agent is intravenously injected, it also has the properties of a hepatocyte-specific agent and thus enables assessment of hepatocellular uptake (17). After intravenous injection, gadoxetic acid distributes into the vascular and extravascular spaces during the arterial, portal, and transitional dynamic phases.

Tumor vascularity can be evaluated in the arterial phase. During the arterial and portal venous phases, there is limited distribution of contrast material in true extracellular spaces. After these phases, the entry of gadoxetic acid into the liver cells causes intense parenchymal enhancement, beginning within 1 or 2 minutes after it is administered. Therefore, there are no true extracellular phases (equivalent to delayed phase with conventional extracellular contrast agent) in gadoxetic acid-enhanced MRI (17).

The period 2–5 minutes after the injection (ie, transitional phase) represents a transition from extracellular-dominant (ie, portal venous phase) to intracellular-dominant (ie, HBP) enhancement (18). Consequently, in the HBP, the liver parenchyma is strongly enhanced. The liver parenchyma and hepatic mass lesions expressing transporters of gadoxetic acid can show uptake early in the transitional phase. This early uptake progresses until it reaches a peak during the HBP. The product information sheet for gadoxetic acid from the manufacturer states that although the HBP can occur within 10–120 minutes after the contrast agent injection, in confirmatory studies most of the data were obtained within 20 minutes after the injection (19). After gadoxetic acid is taken up by hepatocytes, it is excreted from these cells into the biliary canaliculi (20). Thus, unlike the extravascular spaces with traditional gadolinium-based contrast agents, the extravascular spaces with gadoxetic acid comprise extracellular space, hepatocellular space, and bile ducts.

During the HBP, normal liver parenchyma appears uniformly bright on T1-weighted MR images because of the accumulation of gadoxetic acid. In addition, contrast enhancement becomes visible in the larger bile ducts, and blood vessels become dark compared with the liver parenchyma (19).

Table 1: Lesions and Mechanisms Causing Hyperintensity during HBP Gadoteric Acid-enhanced MRI

Hyperintensity-causing Mechanism*	Reported Prevalence or Incidence [†]	Degree of Hyperintensity
Uptake by hyperplastic normal hepatocytes		
FNH	0.9% (4)	Moderate to marked
FNH-like lesion	3.4% of cirrhotic livers (7)	Moderate to marked
NRH	2.6% of cases in autopsy series (8)	Moderate to marked
Uptake by tumor cells		
HCA	Three to four of 100 000 persons (9)	Mild to moderate
HCC	6.2 cases in 100 000 persons (10)	Mild to moderate
Retention in extracellular space		
Fibrotic tumor	NA	Minimal to moderate
Cavernous hemangioma	≤20% (11)	Minimal to moderate
Peritumoral retention		
HCC	6.2 cases in 100 000 persons (10)	Minimal to marked
GIST	54% of metastatic GISTs (12)	Minimal to marked
NET	82% of metastatic NETs (13) Rare in primary tumors	Minimal to marked
Biliary tract enhancement		
IPNB	Rare	Marked
Malignant lymphoma	Primary: <1% of extranodal lymphomas (14) Secondary: 15% of stage IV lymphomas (15,16)	Marked

*Uptake and retention refer, respectively, to the uptake or retention of gadoteric acid. FNH = focal nodular hyperplasia, GIST = gastrointestinal stromal tumor, HCA = hepatocellular adenoma, HCC = hepatocellular carcinoma, IPNB = intraductal papillary neoplasm of the bile duct, NET = neuroendocrine tumor, NRH = nodular regenerative hyperplasia.

[†]Reference numbers for the studies from which the data were taken are in parentheses. NA = not applicable.

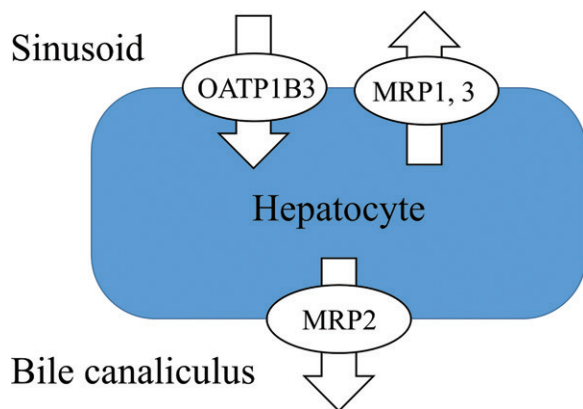


Figure 1. Drawing illustrates the mechanisms of transport of gadoteric acid in hepatocytes. OATP1B3 expressed at the sinusoidal membrane is a major uptake transporter of gadoteric acid. MRP1 and MRP3 expressed on the sinusoidal side and MRP2 expressed on the canalicular side are export transporters of gadoteric acid.

Transporters of Gadoteric Acid

Organic anion-transporting polypeptide 1B3 (OATP1B3) expressed at the sinusoidal membrane in human hepatocytes is considered to be a major uptake transporter of gadoteric acid (21). Multidrug resistance-associated protein (MRP) 1 and MRP3 expressed on the sinusoidal side and

MRP2 expressed on the canalicular side are export transporters of gadoteric acid (22) (Fig 1). For hepatic mass lesions, a significant correlation between the signal intensity of these lesions during the HBP and their OATP1B3 expression has been reported (23,24). On the other hand, the influence of MRPs on HBP findings is considered to be minimal (4). Because mass lesions without functioning hepatocytes commonly exhibit low or no OATP1B3 expression, they are hypointense relative to the background liver tissue during the HBP. Gadoteric acid-enhanced MRI has been proven to have higher sensitivity in the detection of hepatic mass lesions because of these features.

Additional molecular-genetic analyses of HCCs have revealed that HCC with hyperintensity during the HBP (ie, OATP1B3-overexpressed HCC) shows β -catenin and hepatocyte nuclear factor 4 α activation (25,26). A similar molecular mechanism of OATP1B3 expression can be expected in other hepatocellular nodules (4).

Gadoteric Acid-enhanced MRI Findings in LI-RADS

The Liver Imaging Reporting and Data System (LI-RADS) standardizes interpretation of the imaging features of hepatic lesions in patients

who are at risk for HCC (18). This system was developed by a committee that is supported by the American College of Radiology and that comprises diagnostic radiologists with expertise in liver imaging. This committee receives valuable input from hepatobiliary surgeons, hepatologists, hepatopathologists, and interventional radiologists (27).

Nonperipheral washout, nonrim arterial phase hyperenhancement, and capsule enhancement are major features of HCC. Nonperipheral washout should be assessed in the later phases—during the portal venous phase of gadoxetic acid-enhanced MRI or during the portal venous phase or delayed phase of conventional extracellular contrast material-enhanced CT or MRI (28). This means that the transitional phase in gadoxetic acid-enhanced MRI cannot be used to evaluate nonperipheral washout. In gadoxetic acid-enhanced MRI, the transitional phase represents transition from the extracellular-dominant phase to the intracellular-dominant phase. With use of other contrast agents, the transitional phase is fundamentally different from the conventional delayed phase, during which enhancement reflects the extracellular distribution of contrast material. In the LI-RADS, the transitional phase rather than the delayed phase is used for gadoxetic acid-enhanced MRI. For this reason, the transitional phase of gadoxetic acid-enhanced MRI is not appropriate for evaluating the presence of washout (18).

Advantages and Disadvantages of Using Gadoxetic Acid

Table 2 summarizes the advantages and disadvantages of using gadoxetic acid as an imaging contrast agent. The primary advantage is improved detection of hepatic masses, especially small lesions (5,6). Another advantage of using gadoxetic acid is that it facilitates diagnosis of borderline hepatic nodules such as dysplastic nodules and early-manifesting HCCs. Early HCCs and approximately one-third of high-grade dysplastic nodules appear as nonhypervascular nodules that demonstrate hypointensity during the HBP (4). Gadoxetic acid can also help to characterize hepatic mass lesions.

The arterial and venous phase enhancement seen with gadoxetic acid has been described as weak compared with that seen with conventional extracellular contrast agents (29). In addition, transient dyspnea (30) and transient severe motion (31) related to gadoxetic acid uptake during the arterial phase have been reported previously. Gadoxetic acid causes imaging artifacts during the arterial phase. In addition, uptake in the liver parenchyma reflects liver function (32) and

Table 2: Advantages and Disadvantages of Using Gadoxetic Acid for MRI

Advantages
High detectability of small lesions during HBP
Useful for diagnosis of borderline lesions (eg, DN and early HCC)*
Useful for characterization of hepatic mass lesions
Disadvantages
Lower arterial phase and venous phase enhancement
Higher frequency of imaging artifacts during arterial phase due to transient dyspnea and/or transient severe motion
Decreased uptake in liver parenchyma due to liver dysfunction and/or fibrosis

*DN = dysplastic nodule.

fibrosis (33), and, thus, the uptake of gadoxetic acid decreases as liver function or fibrosis worsens. These disadvantages of gadoxetic acid can decrease diagnostic accuracy and overall sensitivity in the detection of hepatic lesions.

Gadoxetic Acid Uptake by Hyperplastic Hepatocytes

Focal Nodular Hyperplasia

FNH is the second most common benign tumor after hemangioma, with a prevalence of 0.9% (4). FNH typically occurs as a solitary lesion in young females. It is usually discovered incidentally in individuals, more commonly women, in their 3rd to 5th decade of life. FNH typically consists of two components: hyperplastic hepatocytes and a central scar. Hyperplastic hepatocytes are considered to be a proliferative response of hepatocytes secondary to an underlying perfusion disorder (34). The central scar is not a true scar; rather, it represents a congeries of blood vessels and bile ducts.

At MRI, findings of FNH typically include areas of peripheral hyperplastic hepatocytes and central scars (Fig 2). The hyperplastic area is slightly hypointense to hyperintense on T1-weighted MR images and isointense to slightly hyperintense on T2-weighted MR images, with intense homogeneous enhancement during the arterial phase (35). In FNH, the presence of fat, which demonstrates signal loss on out-of-phase gradient-echo MR images compared with the signal intensity seen on in-phase images, is extremely rare (36). The majority of hyperplastic areas are isointense or hyperintense relative to the surrounding liver tissue during the HBP. This finding enables differential diagnosis (37)

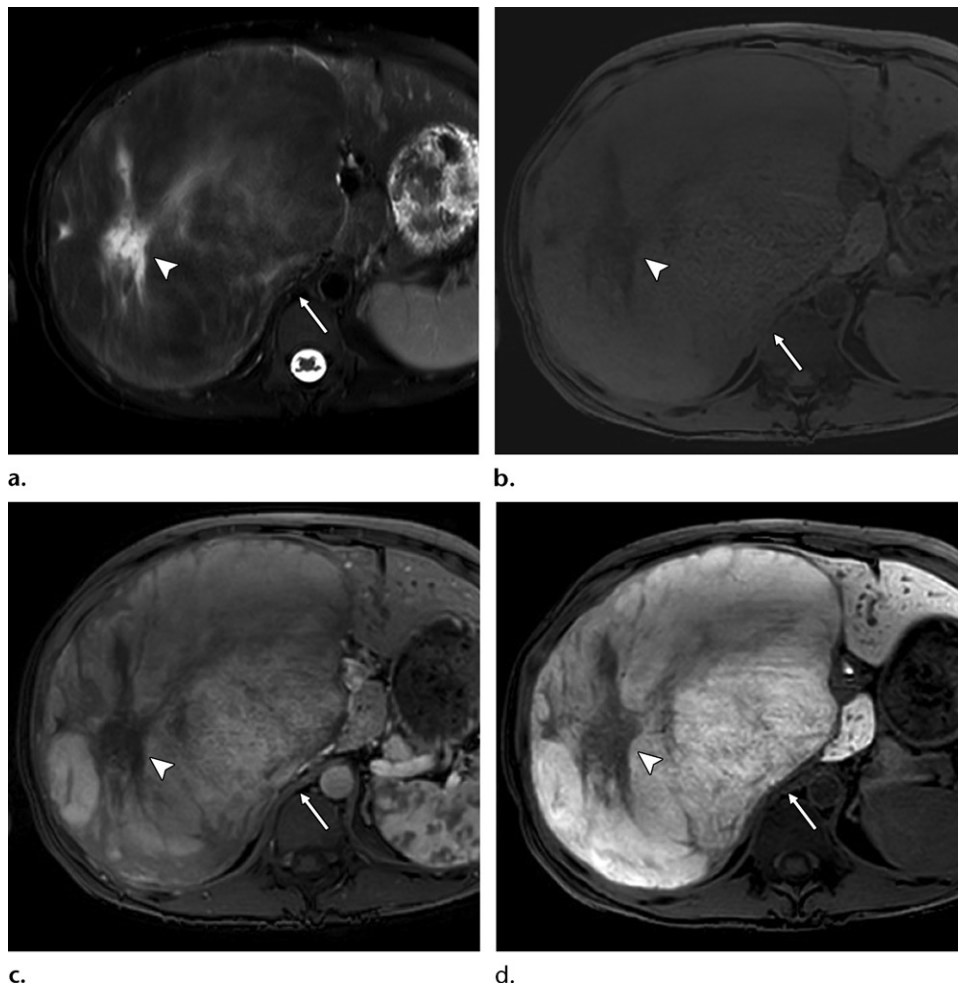


Figure 2. Typical MRI findings of FNH in a 19-year-old woman. **(a)** Axial T2-weighted MR image shows an isointense hyperplastic area (arrow) and a hyperintense central scar (arrowhead). **(b)** Axial T1-weighted MR image shows a slightly hyperintense hyperplastic lesion (arrow) and a hypointense central scar (arrowhead). **(c)** Axial arterial phase T1-weighted MR image shows enhancement of the hyperplastic area (arrow) and nonenhancement of the central scar (arrowhead). **(d)** On the axial HBP MR image, the hyperplastic area (arrow) is hyperintense and the central scar (arrowhead) is hypointense.

because most hypervascular liver masses show hypointensity during the HBP.

Hyperplastic hepatocytes represent a nonneoplastic condition that involves normal functioning hepatocytes and abnormal bile ducts that do not communicate with the normal surrounding biliary system. These characteristics account for the uptake of gadoteric acid in functioning hepatocytes in FNH and the isointensity or hyperintensity during the HBP (38). On the other hand, the central scar is usually hyperintense at T2-weighted MRI (35) and hypointense during the HBP because it contains no or few functioning hepatocytes (24). Therefore, the imaging findings of FNH during the HBP include ring or doughnut-like enhancement (4,39).

FNH has various imaging appearances, depending on the proportions of peripheral hyperplastic areas and central scars (Figs 3, 4). In addition, in FNH, especially that involving lesions

smaller than 3 cm, macroscopic central scars are often absent (40). Thus, it is not rare for small FNH lesions to show uniform iso- or hyperintensity during the HBP. Mohajer et al (41) reported that almost 40% of FNH lesions showed uniform iso- or hyperintensity and almost 60% of FNH lesions showed ring or doughnut-like enhancement during the HBP.

There is an equal or stronger expression of OATP1B3 in FNH compared with that in the background liver tissue, and this expression correlates with the isointensity or hyperintensity seen during the HBP (24). In contrast, no somatic mutations in the β -catenin, *TP53*, *APC*, or *HNF1 α* gene have been identified at genetic analysis of FNH (4). The researchers in one study (42) found that FNH showed activation of the Wnt/ β -catenin pathway without any mutations in the gene that encodes β -catenin. Such a molecular mechanism might explain the equal or stronger

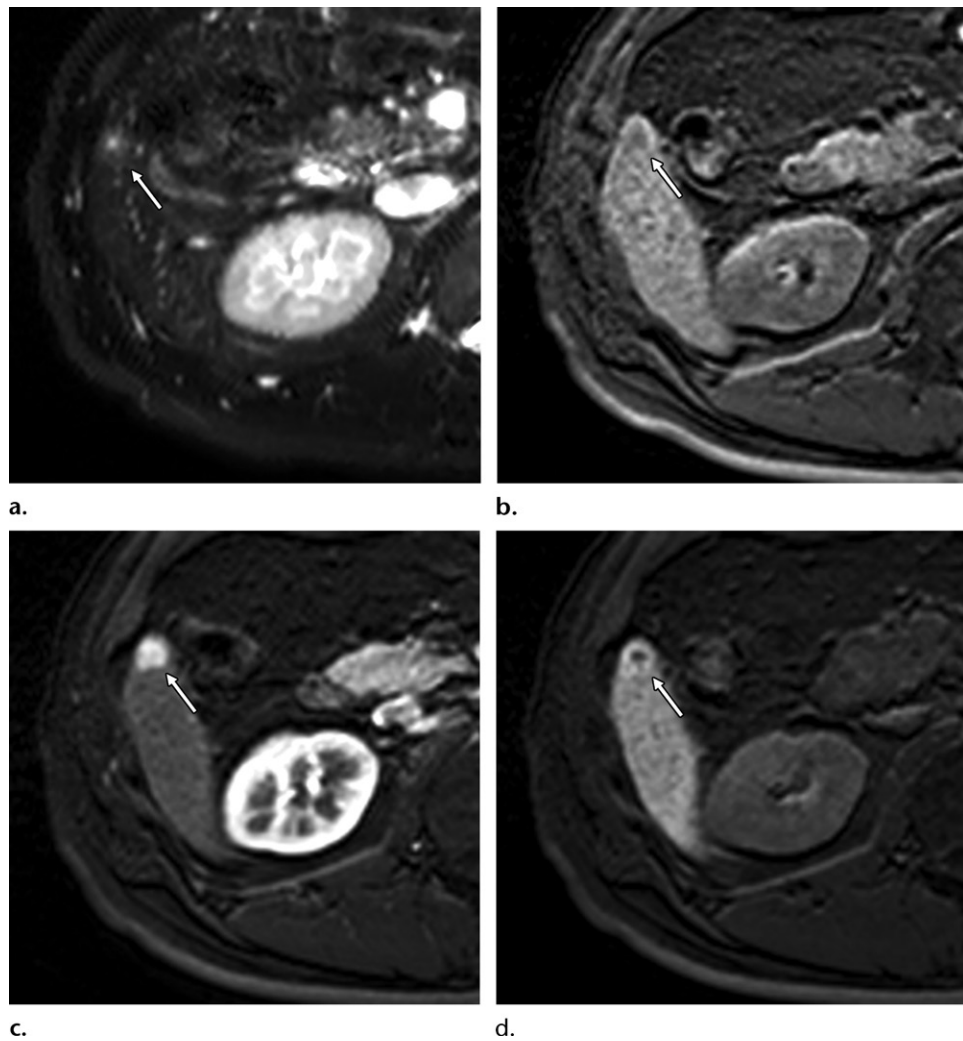


Figure 3. Small FNH lesion with a small central scar in a 37-year-old man. (a) Axial T2-weighted MR image shows a slightly hyperintense lesion (arrow) with a small hyperintense central scar. (b) Axial T1-weighted MR image shows the lesion (arrow) with slight hypointensity. (c) Axial arterial phase T1-weighted MR image shows enhancement of the entire lesion (arrow). (d) Axial HBP MR image clearly shows a peripherally hyperintense hyperplastic area with a hypointense central scar (arrow).

OATP1B3 expression and hyperintensity of FNH during the HBP.

The differential diagnosis of incidental hypervascular liver masses includes HCC, hemangioma, and HCA (37). Differentiating HCC from FNH is important for selecting the appropriate treatment and avoiding unnecessary interventions. Typical FNH occurs in the noncirrhotic liver. In contrast, HCC commonly occurs in persons with chronic liver disease. An enhancing capsule, nonperipheral washout, and threshold growth are typical of HCC (43). A hypointense rim during the HBP, like the appearance of a capsule at gadoteric acid-enhanced MRI, could improve detection of the tumor capsule and the subsequent diagnosis (44).

HCC demonstrating hyperintensity during the HBP, as compared with hyperintense FNH, is not common (10%–15% of cases) (45,46). However, in the LI-RADS, HBP hyperintensity

is not included as a feature of benignity. Thus, the diagnosis must be based on primary features (43). HCC occasionally contains fat, and fat in a mass is one of the ancillary features favoring a diagnosis of HCC in the LI-RADS (47).

Fibrolamellar HCC is an uncommon type of HCC that affects young adults. It frequently appears as a large well-demarcated lobulated liver mass that may contain a scar and calcifications. A fibrolamellar HCC scar demonstrates hypointensity at T2-weighted MRI (17). In addition, fibrolamellar HCC is hypointense, as compared with the background liver parenchyma, during the HBP (17,48).

Hemangiomas show well-known peripheral nodular enhancement with centripetal progression at dynamic CT and MRI performed with extracellular contrast agents. It has been reported that lesion isointensity or hyperintensity during the HBP is accurate for distinguishing FNH from HCA (37). However, McInnes et al (49) reported

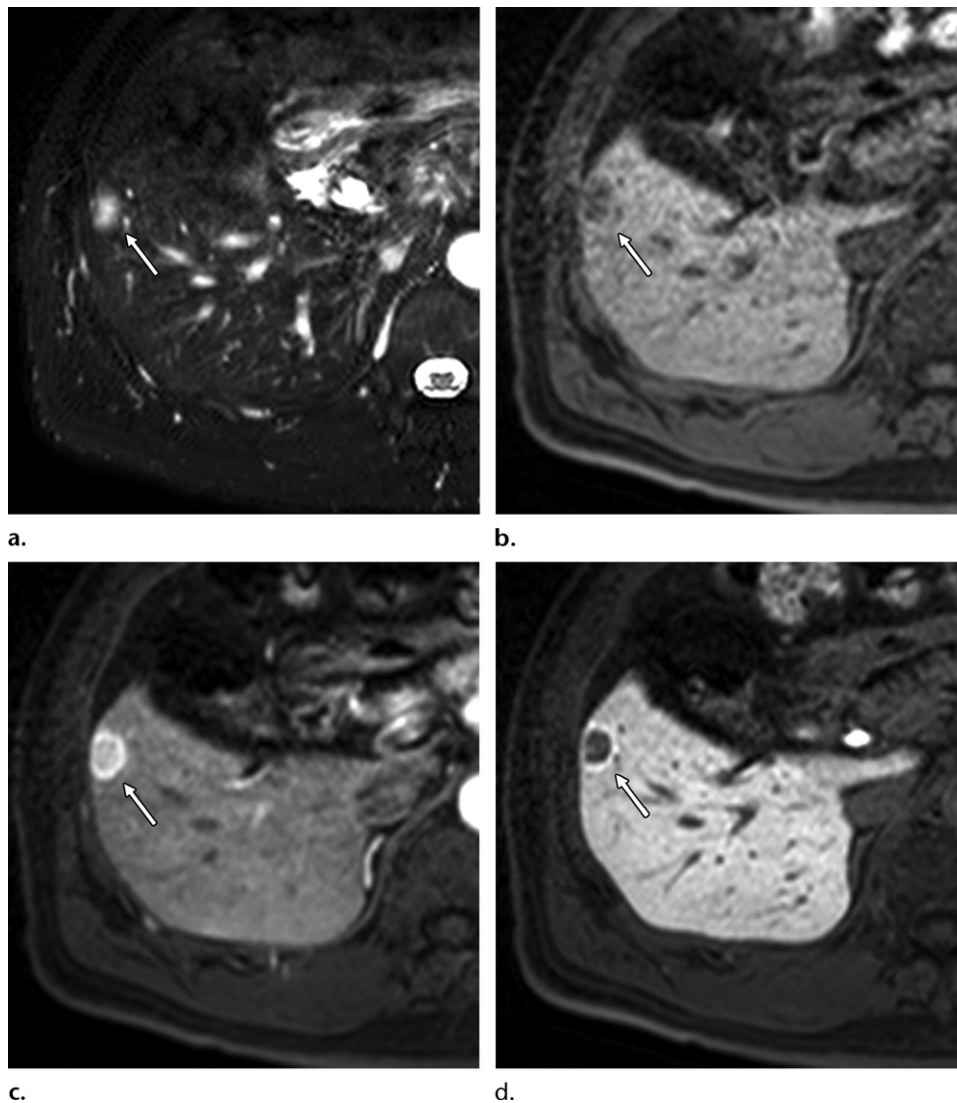


Figure 4. Small FNH with a large central scar in a 65-year-old man. (a) Axial T2-weighted MR image shows a large hyperintense central scar with a small mildly hyperintense peripheral hyperplastic area (arrow). (b) Axial T1-weighted MR image shows the lesion (arrow) with slight hypointensity. (c) Axial arterial phase T1-weighted MR image shows the lesion (arrow) with intense peripheral enhancement and the central scar with mild enhancement. (d) Axial HBP MR image shows a hyperplastic area (arrow) with peripheral hyperintensity and a large hypointense central scar.

that the previously reported high accuracy of HBP findings might be overestimated.

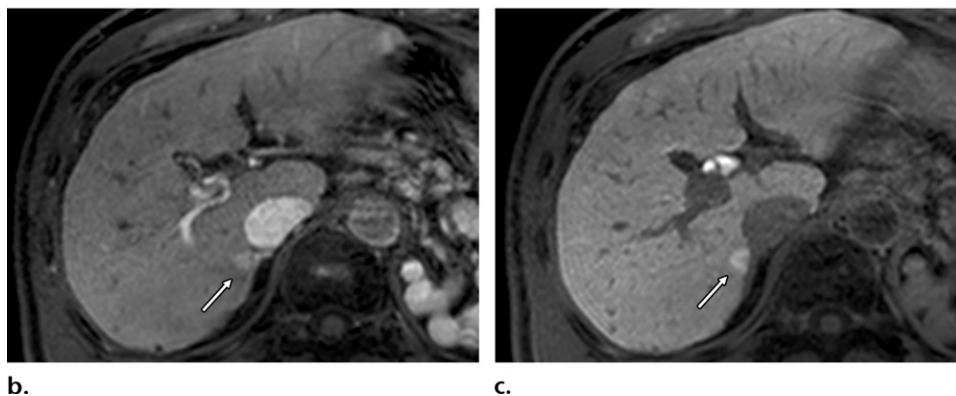
FNH-like Lesions

An FNH-like lesion is a benign lesion that manifests in cirrhotic livers, cases of alcoholic liver cirrhosis especially (50). FNH-like lesions are observed in 3.4% of cirrhotic livers (7). They are considered to result from acquired hyperplastic responses to cirrhosis-related vascular alterations (17). In noncirrhotic livers, FNH-like lesions have been reported to be histopathologically indistinguishable from FNH (7). Therefore, the imaging findings of FNH-like lesions are similar to those of FNH. In the cirrhotic liver, an FNH-like lesion, similar to FNH, is considered to be benign. However, studies have

revealed that some FNH-like nodules—specifically, serum amyloid A–positive hepatocellular neoplasms—have the histopathologic features of inflammatory HCA (I-HCA) and that some have neoplastic features that are similar to those of HCA (51). Further investigation of these findings is needed.

At MRI, FNH-like lesions are isointense or mildly hyperintense on T1-weighted images and mildly hyperintense on T2-weighted images, with arterial phase hyperenhancement. If a central scar is present, it is hyperintense on T2-weighted MR images. Like FNH, FNH-like lesions are usually iso- to hyperintense during the HBP (Fig 5). In addition, similar to FNH, FNH-like nodules show equal or stronger OATP1B3 expression compared with the background liver tissue (24).

Figure 5. FNH-like lesion in a 57-year-old man with hepatitis B-related cirrhosis. **(a)** Axial T1-weighted MR image shows a lesion (arrow) with slight hyperintensity. **(b)** Axial arterial phase T1-weighted MR image shows enhancement of the lesion (arrow). **(c)** Axial HBP MR image shows the lesion (arrow) with hyperintensity.



The majority of cirrhosis-related nodules exhibit regenerative changes without cellular atypia; these nodules are termed *regenerative nodules*. Regenerative nodules typically are isointense to hyperintense on T1-weighted MR images and isointense to hypointense on T2-weighted MR images. On dynamic MR images, regenerative nodules show enhancement similar to that of the adjacent liver, and during the HBP, they are isointense. Lipid-containing and steatotic nodules display a loss of signal on out-of-phase gradient-echo MR images compared with their signal intensity on in-phase MR images. Iron-containing and siderotic nodules appear markedly hypointense on T2- and T2*-weighted MR images (17).

Dysplastic nodules also are usually detected in cirrhotic and chronically damaged livers. High-grade dysplastic nodules with clonal features are categorized as premalignant lesions and frequently progress to HCCs. The imaging findings of dysplastic nodules at T1- and T2-weighted MRI are similar to those of regenerative nodules. Also, dysplastic nodules show no definite enhancement during the arterial dominant phase, but they are commonly iso- or hyperintense relative to the surrounding liver tissue during the HBP. However, one-third of high-grade dysplastic nodules can appear as hypointense nodules with decreased OATP1B3 expression (4).

An important differential diagnosis of FNH-like lesion is HCC because both of these tumors

occur in cirrhotic livers. Hyperintensity during the HBP is characteristic of FNH-like lesions. In addition, the presence of a central scar favors the presence of an FNH-like lesion. An enhancing capsule, nonperipheral washout, and threshold growth are typical of HCC (43). Other ancillary imaging features, such as nodule-in-nodule architecture, fat in a mass, corona enhancement, and restricted diffusion, also favor a diagnosis of HCC (47). However, while most FNH-like lesions exhibit hyperintensity during the HBP, these lesions may show portal venous phase washout and hypointensity during the HBP, mimicking HCC. In equivocal cases, close follow-up or biopsy should be considered (17).

Nodular Regenerative Hyperplasia

NRH commonly manifests in normal liver parenchyma. The prevalence of NRH has been reported as 2.6% in autopsy series (8), and this entity is considered to be a response of hepatocytes secondary to the underlying portal blood flow. NRH is characterized by diffuse hyperplastic nodules, commonly 1–3 mm in size, and hepatocytes in the absence of fibrosis (8). It is often associated with underlying systemic diseases, including lymphoproliferative and myeloproliferative disorders, autoimmune diseases, drug exposure, and Budd-Chiari syndrome. Although NRH is a distinct entity from cirrhosis-related regenerative nodules, it also has been associated with portal hypertension (52).

Table 3: Imaging Characteristics of HCA Subtypes

Subtype	Gadoxetic Acid Uptake*	Typical Imaging Finding	Complication
B-HCA	>80%	Gadoxetic acid uptake	Highest risk for malignant transformation
I-HCA	26%–33%	Hyperintense at T2-weighted MRI	Highest risk for hemorrhage
H-HCA	Rare	Intratumoral fat	Least aggressive subtype
U-HCA	Rare	NA	NA

Note.—NA = not applicable.

*Data are the percentages of the given HCA subtype that take up gadoxetic acid.

Because NRH is supplied by portal blood flow, it is hypointense during the arterial dominant phase, shows mild to moderate enhancement during the portal venous phase, and is isointense during the delayed phase (4). NRH may manifest as hypo-, iso-, or hyperintense regions on T1- and T2-weighted MR images (52). In the HBP, NRH shows hyperintensity, with relative hypointensity in the central region of the lesion; this finding is seen as ring or doughnut-like enhancement. The hyperintense portion corresponds to hyperplastic hepatocytes that express OATP1B3, and the central hypointense portion corresponds to the portal tracts (4).

Gadoxetic Acid Uptake by Tumor Cells

Hepatocellular Adenoma

HCA is a rare benign tumor of the liver. Most HCAs occur in young women. The incidence of these tumors is three to four of 100 000 persons in Europe and the United States (9). Oral contraceptive use; androgenic steroid use; and other conditions such as familial diabetes mellitus, galactosemia, and glycogen storage disease type 1 are known risk factors of HCA (52). In addition, persons with HCA are at risk for hemorrhage and malignant transformation (52). Surgical resection is recommended for patients who have an HCA tumor 5 cm or larger or hemorrhage (53).

The imaging findings of HCA at MRI have been well described (4,35). On T1-weighted MR images, HCA can demonstrate areas of high signal intensity. Fat is the main element responsible for the hyperintensity of adenoma seen on T1-weighted MR images. Areas of internal subacute hemorrhage are markedly hyperintense on T1-weighted MR images. Chemical shift MRI can be performed to confirm the fat content, with a decrease in tumor signal intensity seen on opposed-phase MR images (36). HCA has a heterogeneous appearance, with areas of hypointensity or hyperintensity at T2-weighted MRI;

demonstrates a blush of enhancement during the arterial phase; and becomes nearly isointense during the later phases of dynamic gadolinium-based contrast material-enhanced MRI.

HCAs have been classified into four distinct subtypes by using the Bordeaux group system, which is based on genotype and phenotype classifications: β -catenin activated HCA (B-HCA), I-HCA, hepatocyte nuclear factor 1 α -mutated HCA (H-HCA), and unclassified HCA (U-HCA) (Table 3) (54,55). The imaging features of these subtypes, including the findings seen during HBP gadoxetic acid-enhanced MRI, have been reported by using this classification (56–63). HCA usually shows hypointensity during the HBP, and this finding facilitates the differentiation of HCA from FNH (38,41,49,64,65). However, study groups (56–63) have reported that some HCAs, especially the B-HCA and I-HCA subtypes, can take up gadoxetic acid.

B-HCA accounts for 15%–18% of all HCAs. Compared with the other HCA subtypes, B-HCA occurs more frequently in men (4). Owing to β -catenin gene mutation, B-HCA has the highest risk for malignant transformation. In addition, B-HCA is the most common HCA subtype that takes up gadoxetic acid. According to previous reports (59,63,66), more than 80% of B-HCA lesions show isointensity or hyperintensity during the HBP (Fig 6). It also has been reported that glutamine synthetase and OATP1B3, which are downstream targets of the Wnt/ β -catenin pathway, are diffusely positive in immunohistochemical studies of B-HCA (4,67). Such preserved or increased OATP1B3 expression has been shown to correlate with the hyperintensity seen during the HBP (63,68). Otherwise, no discriminant characteristics of the lesion pattern of B-HCA have been found.

I-HCA is the most common subtype of HCA, accounting for 40%–55% of these tumors. I-HCA most commonly occurs in young women and sometimes occurs in men. Obesity and

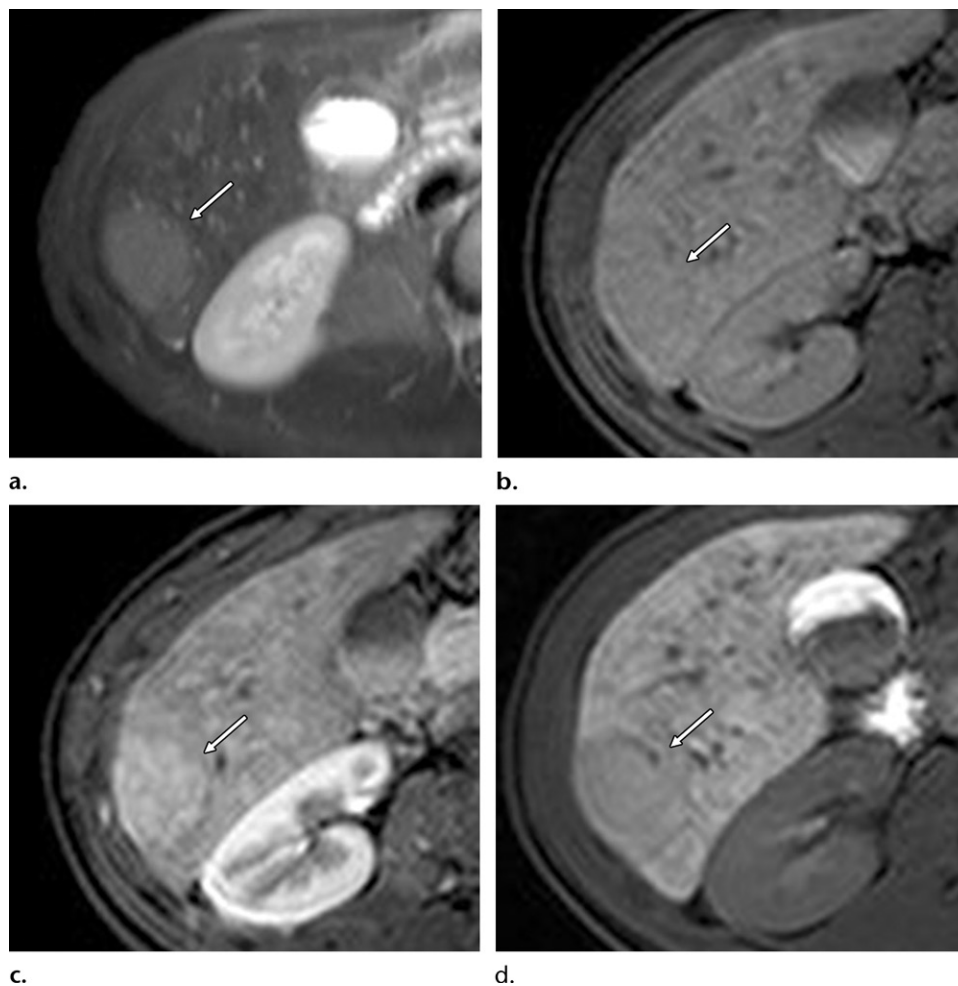


Figure 6. B-HCA in a 14-year-old girl. (a) Axial T2-weighted MR image shows a mildly hyperintense mass (arrow). (b) Axial T1-weighted MR image shows the lesion (arrow) to be isointense. (c) Axial arterial phase T1-weighted MR image shows mild enhancement of the lesion (arrow). (d) Axial HBP MR image shows the lesion (arrow) to be isointense relative to the surrounding liver tissue, indicating the uptake of gadoxetic acid.

alcohol intake are risk factors for I-HCA (4). This HCA subtype has the highest risk for hemorrhage (53). The neoplastic hepatocytes show strong and diffuse expression of the acute phase inflammatory reactants serum amyloid A and C-reactive protein (53).

I-HCA is the second most common HCA subtype that takes up gadoxetic acid. According to previous reports (56,59,62), 26%–33% of I-HCA lesions are isointense or hyperintense during the HBP. In addition, it has been reported that approximately 20% of I-HCAs show β -catenin activation (55). Thus, I-HCAs with β -catenin activation might show expression of OATP1B3 and hyperintensity during the HBP. Moreover, marked hyperintensity at T2-weighted MRI due to sinusoidal dilatation has been found to be typical of I-HCA, with a sensitivity of 85.2% and a specificity of 87.5% (Fig 7) (57). The signal intensity pattern of I-HCA at T2-weighted MRI includes global sinusoi-

dal dilatation and the atoll sign (69,70), which refers to a characteristic hyperintense rimlike band at the periphery of the lesion (70).

H-HCA constitutes 25%–50% of all HCAs, occurs predominantly in women who use oral contraceptives, and often involves multiple nodules (4). Liver-type fatty acid-binding protein, whose expression is controlled by hepatocyte nuclear factor 1 α , is lost in H-HCA tumor cells and is used immunohistochemically to identify H-HCA (53). H-HCA is the least aggressive HCA subtype; individuals with tumors smaller than 5 cm have minimal risk of complications (53). H-HCA usually does not show uptake of gadoxetic acid (59,60). The typical imaging finding of H-HCA is a homogeneous or heterogeneous intratumoral fatty component that shows signal loss during the opposed phase of T1-weighted MRI (59,69,70).

U-HCA constitutes approximately 10% of HCAs. A lesion is assigned to this subtype by

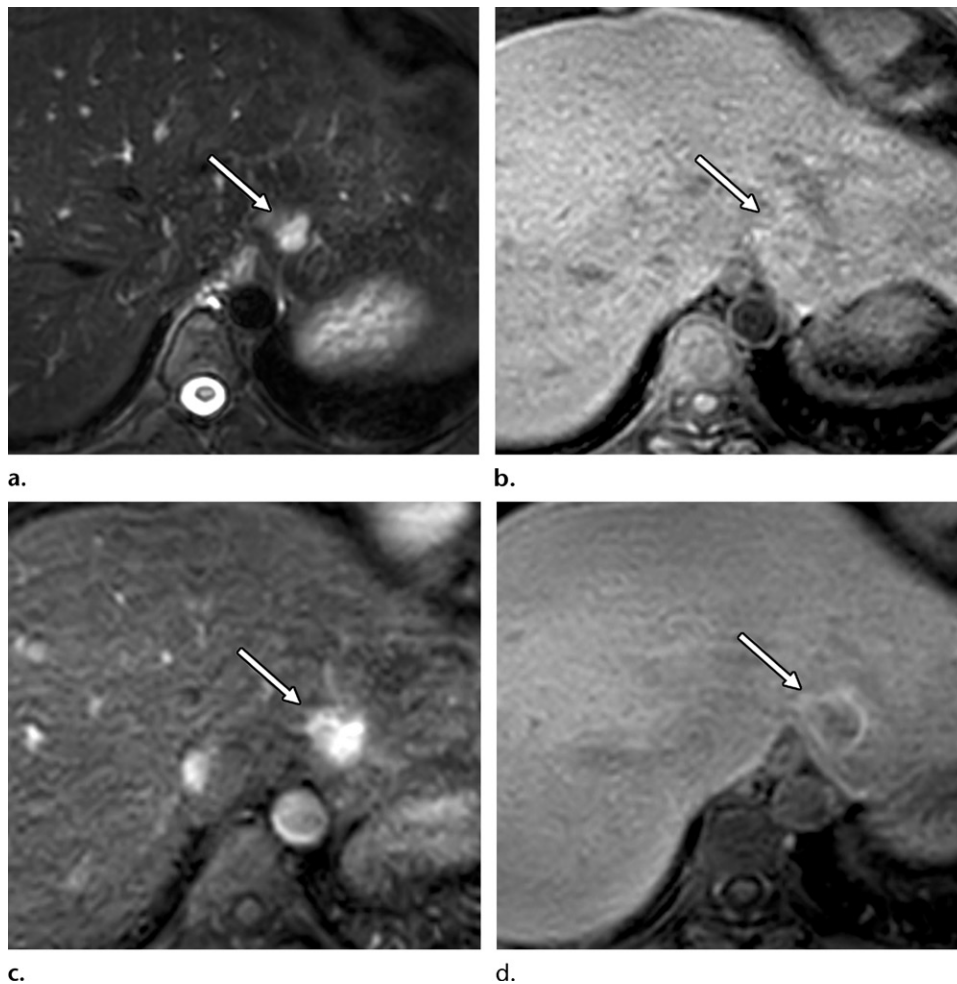


Figure 7. I-HCA in a 33-year-old woman. (a) Axial T2-weighted MR image shows a hyperintense mass (arrow). (b) On the axial T1-weighted MR image, the lesion (arrow) is isointense. (c) Axial arterial phase T1-weighted MR image shows enhancement of the lesion (arrow). (d) Axial HBP MR image shows the lesion (arrow) with peripheral hyperintensity, indicating uptake of gadoxetic acid.

default, when it is negative for all of the features known for the other subtypes, including their immunohistochemical markers (53). U-HCA usually does not show uptake of gadoxetic acid (59). We have found no other specific MRI characteristics of U-HCA. Relatively recently, an additional subgroup of U-HCAs has been described: Sonic hedgehog HCA is characterized by activation of the sonic hedgehog pathway (71). This subgroup is associated with histologically detected hemorrhage and overexpression of argininosuccinate synthase 1 (71,72). Given the clinical importance of hemorrhage, further studies of U-HCAs are required.

It has been reported that distinct imaging characteristics of HCA versus FNH during the HBP of gadoxetic acid-enhanced MRI, with HCA being hypointense and FNH being iso- or hyperintense, have high diagnostic accuracy in the differentiation of these two lesion types (38,41,49,64,65). However, study investigators have reported that this diagnostic accuracy may be overestimated, especially for B-HCA and

I-HCA (49,61). Agarwal et al (56) reported that I-HCA can mimic FNH during the HBP. In addition, the entity previously termed *telangiectatic focal nodular hyperplasia* is now thought to represent I-HCA (55). Given that the classification of HCA subtypes requires immunohistochemical testing that has only recently been part of routine pathologic assessment, further imaging studies with consideration of the more recent classifications of HCAs are needed. The imaging features of benign lesions seen during the HBP are summarized in Table 4.

Hepatocellular Carcinoma

HCC is the fifth most common neoplasm in the world and the most common primary malignant hepatic tumor (73). The prevalence of HCC is 6.2 cases in 100 000 persons in the United States (10). Underlying chronic hepatitis or cirrhosis that is related to hepatitis B virus, hepatitis C virus, alcoholism, or nonalcoholic steatohepatitis is a risk factor. Accurate detection of HCC is one of the

Table 4: Findings of Benign Lesions Seen during HBP MRI

Lesion	Imaging Finding(s)
FNH	Uniform iso- or hyperintensity (40% of cases) Ring or doughnut-like enhancement (60% of cases)
FNH-like lesion	Similar to those of FNH
NRH	Ring or doughnut-like enhancement
Dysplastic nodule	Iso- or hyperintensity, with hypointensity in one-third of high-grade dysplastic nodules
B-HCA	Iso- or hyperintensity (>80% of cases)
I-HCA	Iso- or hyperintensity (30% of cases)

most important components in the management of patients with such chronic liver disease.

Gadoxetic acid-enhanced MRI has become an important imaging modality for diagnosing HCC, with high accuracy due to the high lesion-to-liver contrast achieved with this modality (74,75). HCCs show arterial phase nonrim hyperenhancement and washout during the portal phase. As described earlier, imaging artifact during the arterial phase caused by transient dyspnea (30) or transient severe motion (31) can affect the sensitivity and specificity of gadoxetic acid-enhanced MRI in the detection of HCC. HCCs without functioning hepatocytes usually are hypointense relative to the background liver tissue during the HBP. In addition, it has been reported that a peritumoral area of decreased uptake during the HBP of gadoxetic acid-enhanced MRI is predictive of microscopic vascular invasion by HCC (76).

Approximately 10%–15% of HCCs are hyperintense during the HBP, and the distinct pathologic and biologic characteristics of hyperintense HCCs have been reported (45,46). In hyperintense HCCs, expression of OATP1B3 (an uptake transporter) is preserved, whereas hypointense HCCs show lower or no OATP1B3 expression. Histopathologically, a pseudoglandular proliferation pattern with bile plugs, also called green hepatoma, is commonly observed in hyperintense HCCs (Fig 8). Moreover, hyperintense HCCs exhibit less malignant behavior compared with hypointense HCCs. Hyperintense HCCs seen during the HBP have had significantly lower recurrence rates than have hypointense HCCs seen during this phase (77,78).

The molecular mechanisms that explain the differences between hyperintense and hypointense HCCs have been demonstrated in relatively recent studies (25,26). It has been reported that activation of β -catenin and hepatocyte nuclear factor 4 α correlates with hyperintense HCCs (25,26).

Kitao et al (26) reported that HCC with β -catenin gene mutation showed higher OATP1B3

expression, a pseudoglandular pattern, bile production, and hyperintensity during the HBP. In addition, investigators in other studies have reported that HCCs with β -catenin gene mutation, as compared with HCCs without this mutation, are associated with accelerated bile production (79), higher OATP1B3 expression (80), and a favorable prognosis (81). The investigators in these studies also reported that both hepatocyte nuclear factor 4 α activation and β -catenin activation correlated with hyperintense HCCs (25).

Hepatocyte nuclear factor 4 α has been shown to suppress hepatocyte proliferation and HCC growth (82) and is the central regulator of bile acid conjugation in hepatocytes (83). Such genetic-molecular study findings can explain the clinical and pathologic differences in HCCs. Given these imaging study developments, gadoxetic acid-enhanced MRI can be an effective imaging method, with findings that serve as biomarkers of HCC that reflect the genetic and molecular background of these tumors, or so-called *radiogenomics*.

FNH and FNH-like lesions are important differential diagnoses of the hyperintense HCC seen during the HBP because they also show iso- or hyperintensity during the HBP. Findings in a previous study (84) indicated that arterial phase hyperenhancement with a washout pattern at dynamic CT and a lower apparent diffusion coefficient are important findings that favor a diagnosis of HCC. Some atypical intrahepatic mass-forming cholangiocarcinomas may be categorized as LR-5 or LR-TIV lesions in the LI-RADS, resulting in a false-positive diagnosis of HCC (85).

Retention of Gadoxetic Acid in the Extracellular Space

Fibrotic Tumors

Gadoxetic acid is a valuable contrast agent in liver MRI because it has the combined properties of liver-specific contrast material and conventional extracellular contrast material (86). Thus, both the hepatocyte-specific phase and the dy-

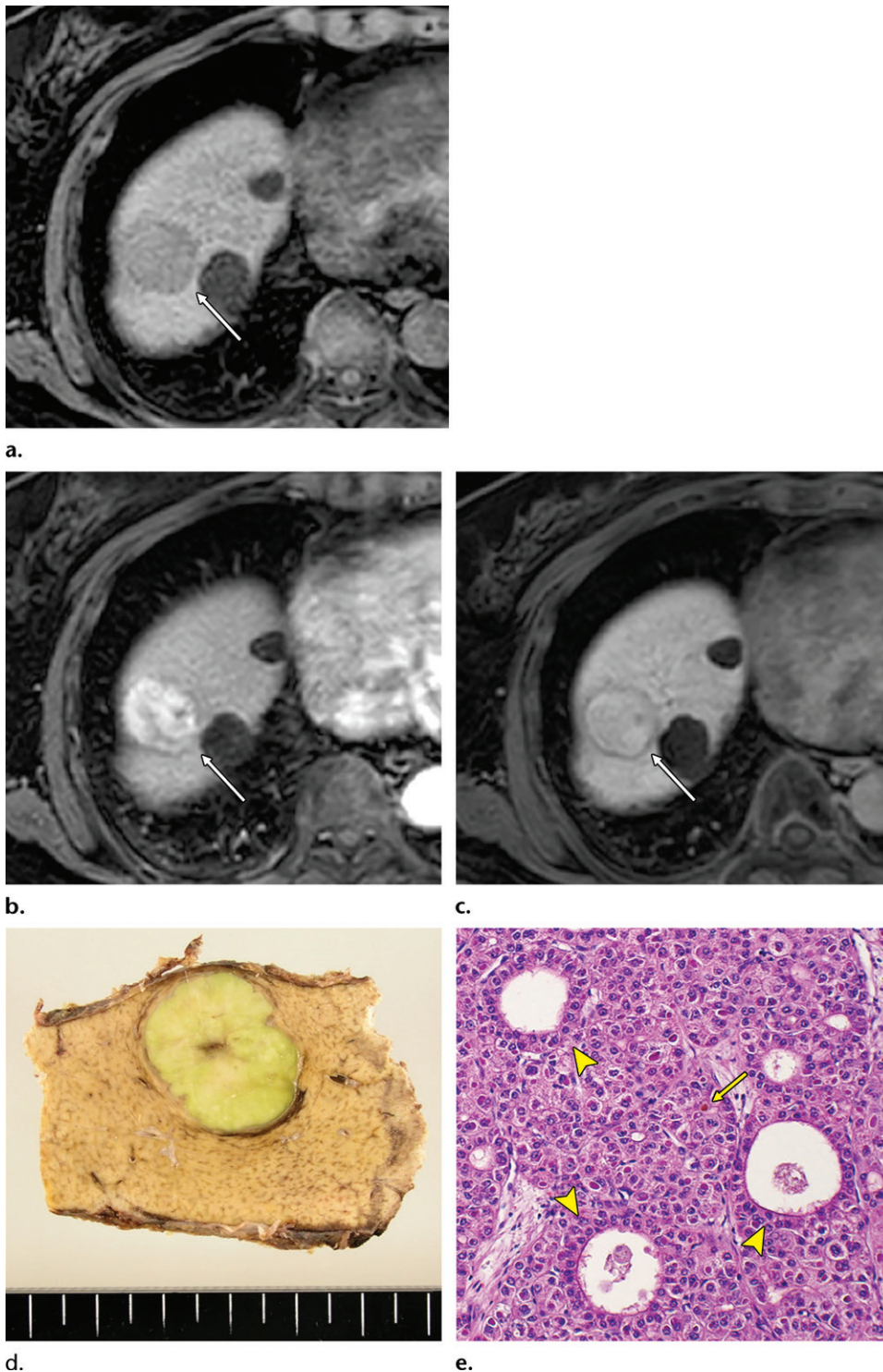


Figure 8. HCC (green hepatoma) in a 79-year-old man with hepatitis B-related cirrhosis. (a) Axial T1-weighted MR image shows a tumor (arrow) with slight hypointensity. (b) Axial arterial phase T1-weighted MR image shows enhancement of the tumor (arrow). (c) On the axial HBP MR image, the tumor (arrow) is hyperintense, indicating uptake of gadoxetic acid. (d) Photograph of the surgically resected specimen shows a greenish nodule. (e) Photomicrograph shows moderately differentiated HCC consisting of pseudoglandular patterns (arrowheads), trabecular patterns, and bile plugs (arrow). (Hematoxylin-eosin stain; original magnification, $\times 200$.)

namic perfusion phase can be evaluated at gadoxetic acid-enhanced MRI. Liver lesions that have expanded extracellular volume, such as fibrosis and necrosis, possibly demonstrate gadoxetic acid

retention in the extracellular space during the HBP owing to the properties of gadoxetic acid that are similar to those of conventional extracellular contrast material.

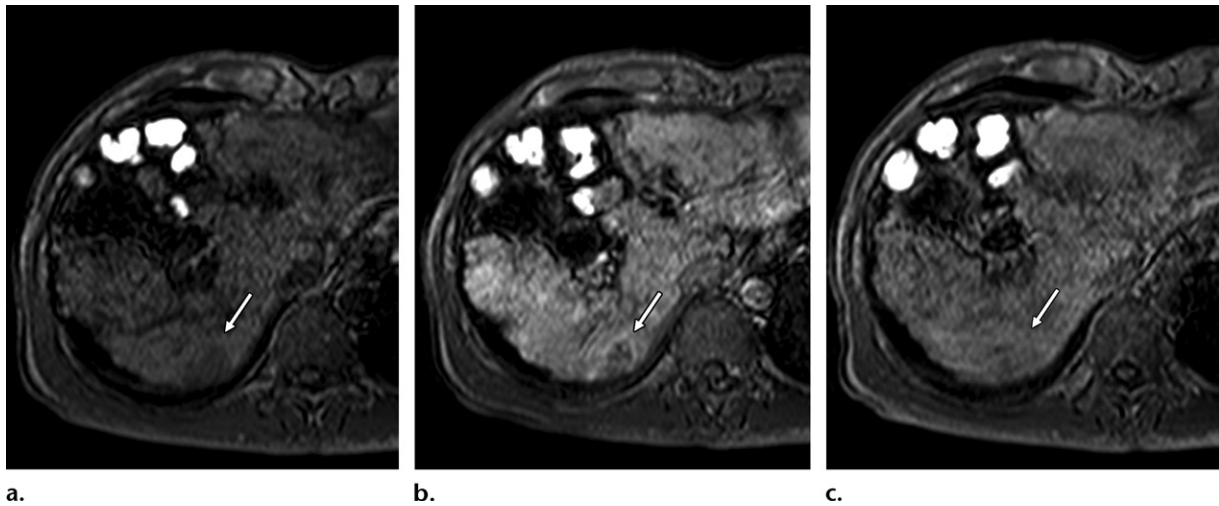


Figure 9. Cholangiocarcinoma in a 53-year-old man. (a) Axial T1-weighted MR image shows the lesion (arrow) with slight hypointensity. (b) Axial arterial phase T1-weighted MR image shows peripheral enhancement of the tumor (arrow). (c) On the axial HBP MR image, the tumor (arrow) is isointense to the surrounding liver parenchyma owing to gadoxetic acid retention in the extracellular space.

It is well known that areas of delayed or prolonged liver tumor enhancement at conventional extracellular contrast-enhanced CT or MRI correspond to fibrotic stroma at histopathologic examination (87). Similarly, liver tumors with fibrous stroma, such as cholangiocarcinoma and metastatic adenocarcinoma, possibly are iso- to hyperintense during the HBP of gadoxetic acid-enhanced MRI because of gadoxetic acid retention in the extracellular space (Fig 9). In previous studies (88,89), almost 80% of cholangiocarcinomas demonstrated gadoxetic acid retention in the extracellular space. In addition, 47%–70% of metastatic carcinomas also show retention of gadoxetic acid in the extracellular space (90–92). Such gadoxetic acid retention in the extracellular space is often observed in the center of the tumor, representing fibrotic stroma or degeneration. Thus, this enhancement pattern during the HBP is referred to as a targetoid pattern.

Despite the retention of gadoxetic acid in the extracellular space, gadoxetic acid-enhanced MRI is useful for detecting metastatic adenocarcinoma (6). Even in the setting of disappearing colorectal metastases after chemotherapy, gadoxetic acid-enhanced MRI is superior to contrast material-enhanced CT in the assessment of these lesions (93).

Park et al (94) reported interestingly that the aberrant expression of OATP1B3 in colorectal cancer liver metastases is associated with mixed hypointensity during the HBP. This finding suggests that the signal intensity of metastatic adenocarcinoma during the HBP may be affected by not only the amount of extracellular tissue but also the aberrant expression of OATP1B3. They also reported that such signal intensity during the HBP was associated with worse survival rates (94). Similarly, patients with colon cancer whose immuno-

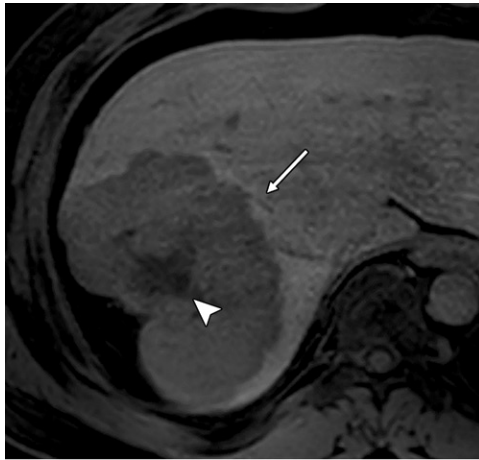
histochemical results indicate OATP1B3 overexpression have worse progression-free survival rates than do patients with scant or negative OATP1B3 expression (95). Given these imaging study developments, gadoxetic acid-enhanced MRI can be an effective imaging method, with findings that serve as biomarkers of metastatic carcinoma and reflect the genetic-molecular background of these tumors (ie, radiogenomics), as well as HCCs.

Some neuroendocrine tumors with a higher fibrous content may show more delayed enhancement that is best visualized during the delayed phase of imaging with extracellular contrast agents (96). Thus, fibrotic neuroendocrine tumors also can show iso- to hyperintensity during the HBP of gadoxetic acid-enhanced MRI (Fig 10). However, such enhancement during the HBP, which is due to retention of gadoxetic acid in the extracellular space, tends to be lower compared with the enhancement related to transporter uptake of gadoxetic acid (17).

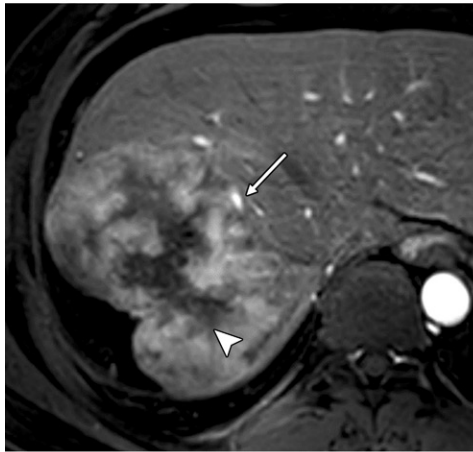
Hemangioma

Hemangioma is the most common benign hepatic neoplasm and is found in less than or equal to 20% of the population (11). Most patients with hemangiomas have no symptoms, but they become symptomatic if the tumor enlarges.

At MRI, hemangioma appears as a well-defined mass. It can have a heterogeneous appearance if there are areas of thrombosis, fibrosis, or degeneration. Markedly hyperintense lesions at T2-weighted MRI are characteristic imaging findings (11). At conventional extracellular contrast-enhanced MRI, hemangiomas typically show peripheral nodular enhancement followed by centripetal enhancement, referred to as filling in, during the later phases (11). The prolonged



a.



b.



c.

Figure 10. Neuroendocrine carcinoma in a 48-year-old man. (a) On an axial T1-weighted MR image, the lesion (arrow) is slightly hypointense, with a central markedly hypointense area (arrowhead). (b) Axial arterial phase T1-weighted MR image shows enhancement of the tumor (arrow), with a central markedly hypointense area (arrowhead). (c) Coronal HBP MR image shows the tumor (arrows) with hyperintense areas owing to the retention of gadoteric acid in the extracellular space. The central hypointense area (arrowhead) correlates with tumor degeneration.

and delayed enhancement is secondary to contrast material entering the multiple vascular channels and slowly filling the lesion (11). This filling in of hemangioma can be seen during the HBP of gadoteric acid-enhanced MRI, reflecting the blood pool, especially when there is sub-optimal clearance of contrast material from the blood pool (Fig 11). Some hemangiomas may show slight central high signal intensity, even during the early HBP beyond the transitional phase (19). Tamada et al (97) reported that 47% of hemangiomas show intratumoral enhancement during the HBP.

High-flow hemangiomas may show relative hypointensity during the transitional phase owing to the uptake of gadoteric acid in the normal surrounding liver parenchyma. This is referred to as the “pseudowashout” sign, which is not considered true contrast material washout, as is seen in HCC (98).

Peritumoral Retention

Peritumoral retention during the HBP of gadoteric acid-enhanced MRI appears as a hyperintense rim surrounding the tumor. This rim is occasionally observed in HCCs (Fig 12). In the Yoneda et al study (99), peritumoral retention with partial enhancement was observed in 50% of HCCs. Histopathologically, peritumoral retention corresponds to *peritumoral hyperplasia*, which is defined as a rim of hyperplastic hepatocytes surrounding the tumor. Peritumoral hyperplasia is also observed in other hepatic tumors, such as neuroendocrine tumors, gastrointestinal stromal tumors, metastatic colon carcinomas, hemangiomas, and hepatoblastomas (100). Thus, these tumors also can show peritumoral retention during the HBP of gadoteric acid-enhanced MRI (Figs 13, 14).

The pathogenesis of peritumoral hyperplasia remains controversial. Perfusion abnormality due to tumor vascular invasion is considered to be

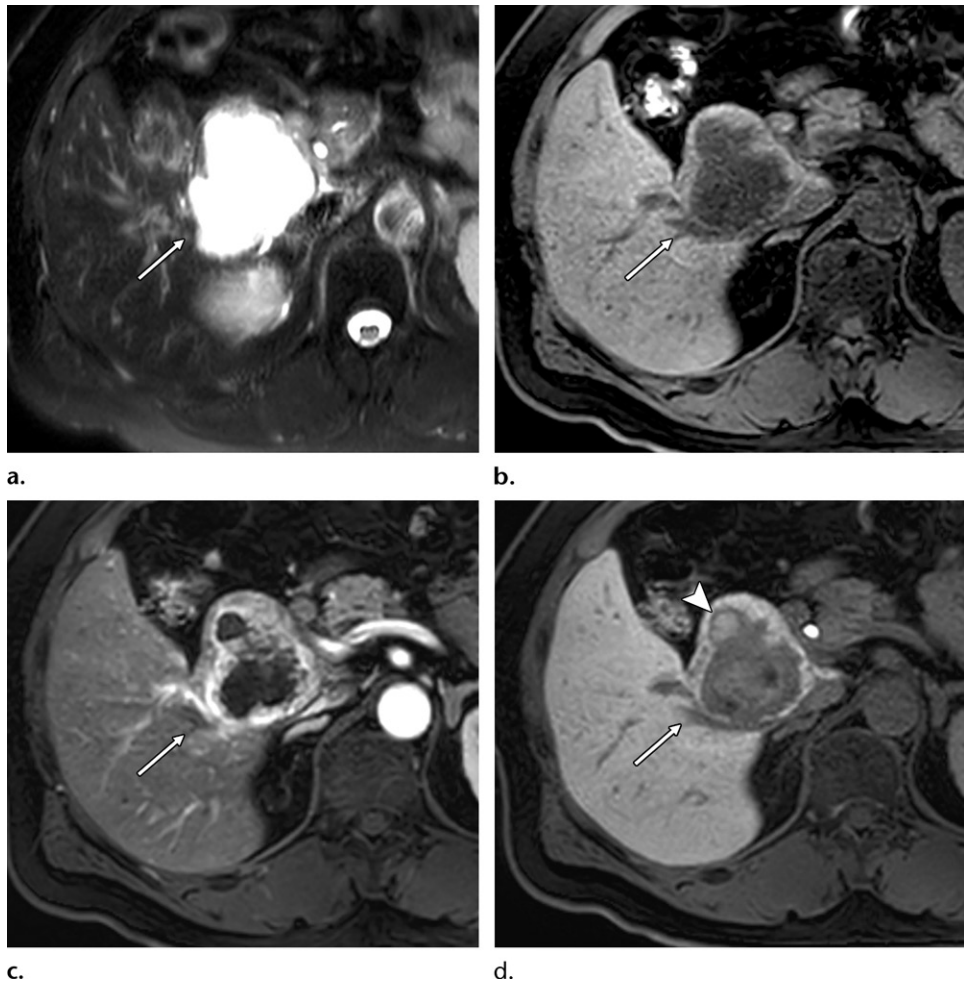


Figure 11. Hemangioma in a 42-year-old man. (a) Axial T2-weighted MR image shows the lesion (arrow) with marked hyperintensity. (b) On an axial T1-weighted MR image, the lesion (arrow) is hypointense. (c) Axial arterial phase T1-weighted MR image shows peripheral enhancement of the lesion (arrow). (d) On an axial HBP MR image, the lesion (arrow) is hypointense, with marked ventral hyperintense foci (ie, filling in) (arrowhead).

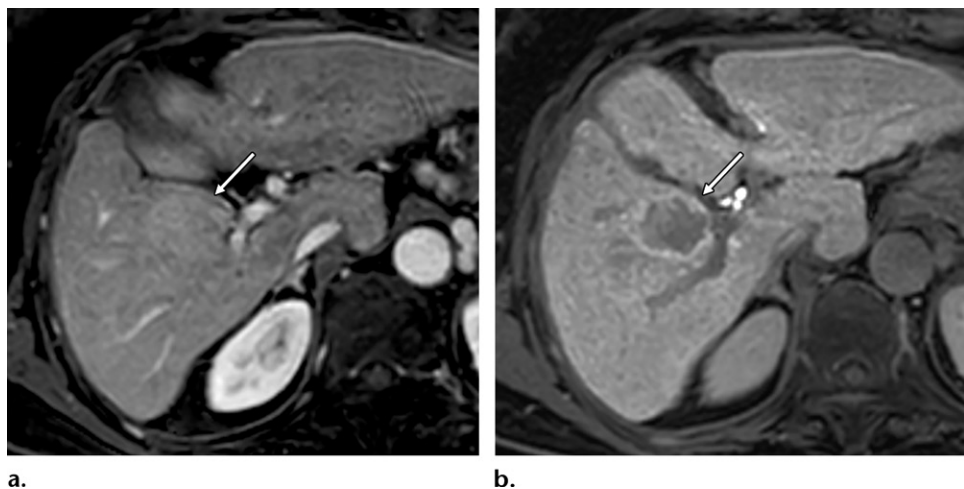


Figure 12. HCC in a 73-year-old woman. (a) Axial arterial phase T1-weighted MR image shows enhancement of the tumor (arrow). (b) On an axial HBP MR image, the lesion (arrow) is hypointense and surrounded by a hyperintense rim, indicating peritumoral retention.

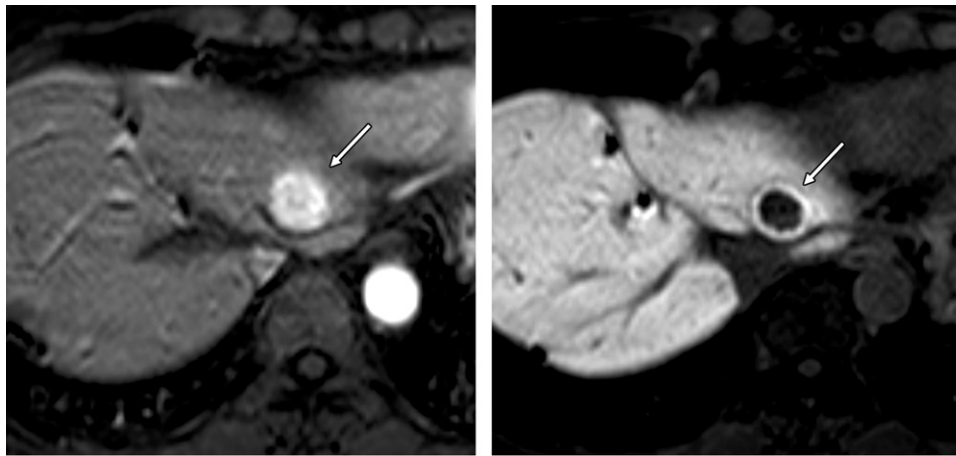


Figure 13. Metastatic gastrointestinal stromal tumor in a 51-year-old woman. (a) Axial arterial phase T1-weighted MR image shows an enhancing tumor (arrow). (b) On an axial HBP MR image, the tumor (arrow) is hypointense, with a hyperintense rim, indicating peritumoral retention.

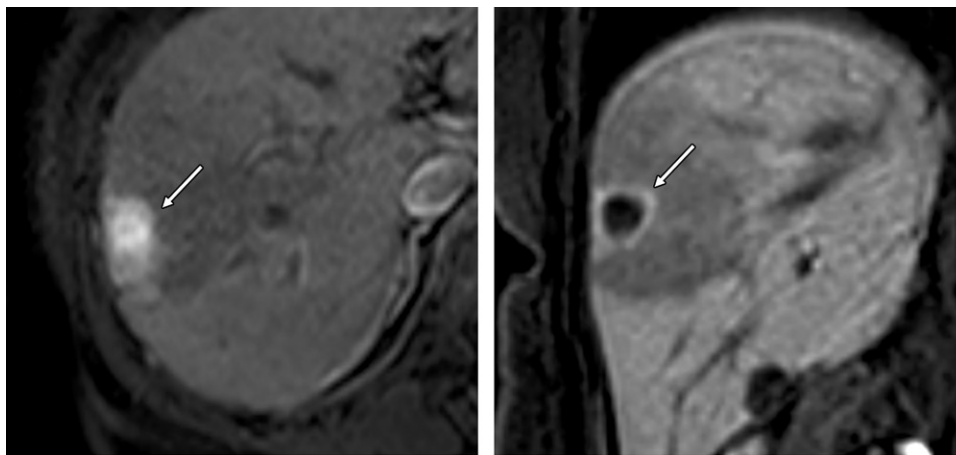


Figure 14. Metastatic neuroendocrine tumor in a 65-year-old woman. (a) Axial arterial phase T1-weighted MR image shows enhancement of the tumor (arrow). (b) On a coronal HBP MR image, the tumor (arrow) is hypointense and surrounded by a hyperintense rim, indicating peritumoral retention.

a major possible cause. Peritumoral hyperplasia is commonly seen in hypervascular neoplasms (100). In addition, portal venous invasion (100) or hepatic venous invasion (99) is more frequently observed in tumors with peritumoral hyperplasia. Such vascular invasion causes increased arterial blood flow in the peritumoral liver parenchyma and consequent hepatocyte hyperplasia.

Another pathogenesis of peritumoral hyperplasia could be regenerative changes in hepatocytes compressed by the tumor (99). Tumors such as HCC, neuroendocrine tumor, and gastrointestinal stromal tumor usually show expansive growth and do not show the type of infiltrative growth seen with adenocarcinomas. Such expansive growth can cause strong compression of the liver parenchyma and regenerative changes of hepatocytes, causing peritumoral retention.

The differential diagnosis of liver tumors that show peritumoral retention includes FNH and FNH-like lesions, which appear as ring or doughnut-like enhancement during the HBP. Peritumoral retention is observed in the adjacent liver parenchyma outside the tumor, while ring or doughnut-like enhancement is observed in the lesion. Precisely recognizing the tumor margin by referring to the findings seen with other sequences is important for differential diagnosis.

Biliary Tract Enhancement

Gadoxetic acid is eliminated in approximately equal proportions by the liver (43.1%–53.2%) and by the kidneys, with renal glomerular filtration and subsequent excretion (41.6%–51.2%) (20). After being taken up by hepatocytes, gadoxetic acid is excreted from these cells into the

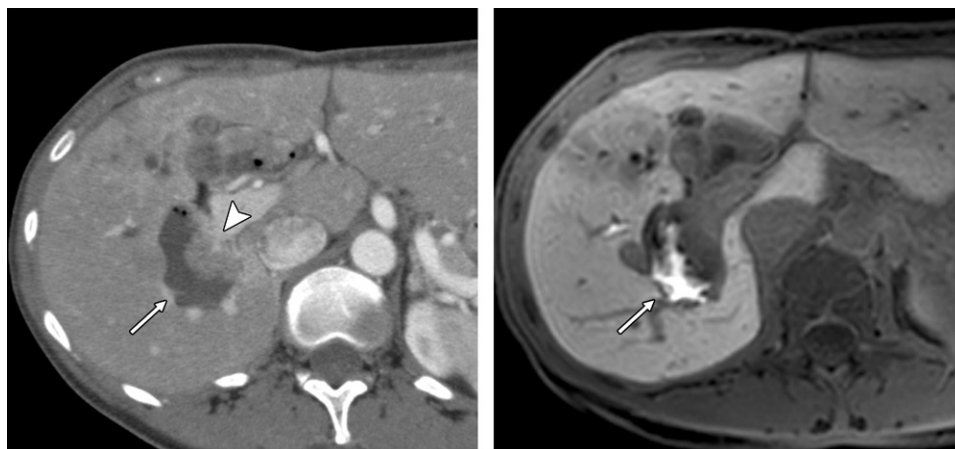


Figure 15. IPNB in a 52-year-old woman. **(a)** Contrast-enhanced CT image shows a cystic tumor (arrow) with a solid component (arrowhead). **(b)** Axial HBP MR image shows the cystic component—that is, the dilated bile duct (arrow)—to be well enhanced.

biliary canaliculi. Excretion into the bile ducts causes biliary luminal enhancement as early as 5–10 minutes after the injection. A 20-minute delay after the gadoxetic acid injection (ie, the HBP) may be sufficient for adequate biliary evaluation (20). Such biliary enhancement during the HBP is sometimes useful for diagnosing hepatic liver mass lesions.

Intraductal Papillary Mucinous Neoplasm of the Bile Duct

IPNB is a subtype of bile duct carcinoma (101). The histopathologic and immunohistochemical features of IPNB are similar to those of intraductal papillary mucinous neoplasms of the pancreas. Thus, IPNB is considered to be a “counterpart” disease of pancreatic intraductal papillary mucinous neoplasms. The imaging findings of IPNB include papillary or polypoid growth of the tumor along the bile duct, with expansive and significant dilatation of the bile duct upstream or downstream of the tumor (102). Dilatation of the bile duct has a cystic appearance and is usually connected with the involved bile ducts (102). For this reason, IPNB is usually diagnosed by using endoscopic retrograde cholangiopancreatography to determine the presence of mucin in the dilated bile duct (103).

The usefulness of gadoxetic acid-enhanced MRI in the diagnosis of IPNB has been reported. During the HBP, IPNB demonstrates a dilated enhanced bile duct with filling defects caused by mucin retention or a solid component of the tumor (Fig 15) (104–106). Note that when there is a large amount of mucin in a bile duct, it results in marked bile duct dilatation and obvious impaired liver function. In this setting, the hepatocellular uptake of gadoxetic acid and secretion

of this agent into the bile duct have obviously decreased and led to nonenhancement of the biliary ducts during the HBP (106). The addition of diffusion-weighted imaging to the gadoxetic acid-enhanced MRI examination has the potential to improve the conspicuity of intraductal tumors in IPNB and is helpful in determining tumor invasiveness (107).

Malignant Lymphoma

Primary lymphoma of the liver is a rare malignant tumor, accounting for fewer than 1% of extranodal lymphomas. In contrast, hepatic extension (ie, secondary malignant lymphoma) in stage IV lymphoma has been observed in 15% of cases (15,16). Primary lymphomas of the liver are mainly large B-cell non-Hodgkin lymphomas. The risk factors for hepatic lymphomas are hepatitis C virus infection, Epstein-Barr virus infection, human immunodeficiency virus infection, and autoimmune disease (15,16).

At MRI, lymphomas of the liver are homogeneously hypointense to isointense on T1-weighted images and hyperintense on T2-weighted images. The signal intensity at T1- and T2-weighted MRI may be heterogeneous owing to foci of hemorrhage and necrosis. T2-hypointense tumors with a peripheral rim of hyperintensity also have been reported. The increased signal intensity around the lesion has been attributed to the inflammatory response elicited by the lymphomatous lesion and the resultant surrounding edema. The highly cellular nature of lymphoma typically results in markedly restricted diffusion. The majority of these lesions demonstrate minimal to no enhancement during all phases. The other pattern is that of enhancement of the lesion rim with a central nonenhancing area, resulting in a target-



Figure 16. Malignant lymphoma in an 83-year-old woman. (a) Axial arterial phase T1-weighted MR image shows enhancement of the tumor (arrow). (b) Coronal HBP MR image shows enhanced nondistorted biliary ducts (arrow) in the tumor.

like appearance of the lesion (108). Vascular structures such as portal and hepatic veins in the tumor, with no distortions in size or direction, are highly suggestive of malignant lymphoma (109). Similarly, nondistorted enhancing biliary ducts in the tumor are useful imaging findings in the diagnosis of malignant lymphoma (Fig 16) (110).

Relative Signal Intensity and Differential Diagnosis of Hyperintense Liver Masses during the HBP

The majority of FNHs, FNH-like lesions, and NRHs are iso- to hyperintense during the HBP because they are composed of nonneoplastic hyperplastic hepatocytes. Therefore, marked hyperintensity can be seen during the HBP.

In addition, these lesions often demonstrate ring or doughnut-like enhancement. The differential diagnosis of those among these lesions that have ring or doughnut-like enhancement includes liver tumors that show peritumoral retention during the HBP. Peritumoral retention corresponds to peritumoral hyperplastic hepatocytes surrounding the tumor; thus, peritumoral retention can also show marked hyperintensity during the HBP. Precise recognition of the tumor margin is important for the differential diagnosis.

Dysplastic nodules may be hyperintense, isointense, or hypointense during the HBP, depending on the grade of malignancy. Unlike HCCs, dysplastic nodules demonstrate no definite enhancement during the arterial dominant phase. Approximately 10%–15% of HCCs are hyperintense during the HBP. B-HCA and I-HCA lesions also can show hyperintensity during the HBP. The differentiation between benign nodules (eg, FNH, FNH-like nodules, and NRH) and tumor lesions (eg, HCC and HCA)

is relatively easy when it is based on imaging features, including hemodynamic findings, and other features, as described earlier. However, differentiating HCC from HCA with use of imaging alone is often difficult. Additional clinical information is necessary for differential diagnosis, and biopsy is sometimes needed when it is difficult to make the differential diagnosis.

The hyperintensity caused by gadoxetic acid retention in the extracellular space tends to be lower compared with the hyperintensity caused by transporter uptake of gadoxetic acid (17). However, some hemangiomas can show strong hyperintensity due to the filling-in phenomenon. Comparison of the imaging findings of conventional extracellular contrast-enhanced CT and MRI is important for the differential diagnosis.

Biliary tract enhancement is caused by the physiologic excretion of gadoxetic acid into the bile ducts and therefore is usually strong. IPNB can show a dilated enhanced bile duct with filling defects caused by mucin retention or a solid component of the tumor. Enhanced nondistorted biliary ducts in the tumor are useful imaging findings in the diagnosis of malignant lymphoma. The differential diagnosis of hyperintense liver masses seen during the HBP is summarized in Figure 17.

Conclusion

Hepatic mass lesions without functioning hepatocytes commonly show hypointensity during the HBP of gadoxetic acid-enhanced MRI. However, it is important to identify the specific causes of hyperintensity seen during the HBP. Understanding these causes is useful not only for precise imaging-based diagnosis but also for understanding the pathogenesis of hepatic mass lesions. In other words, gadoxetic acid-enhanced MRI has a

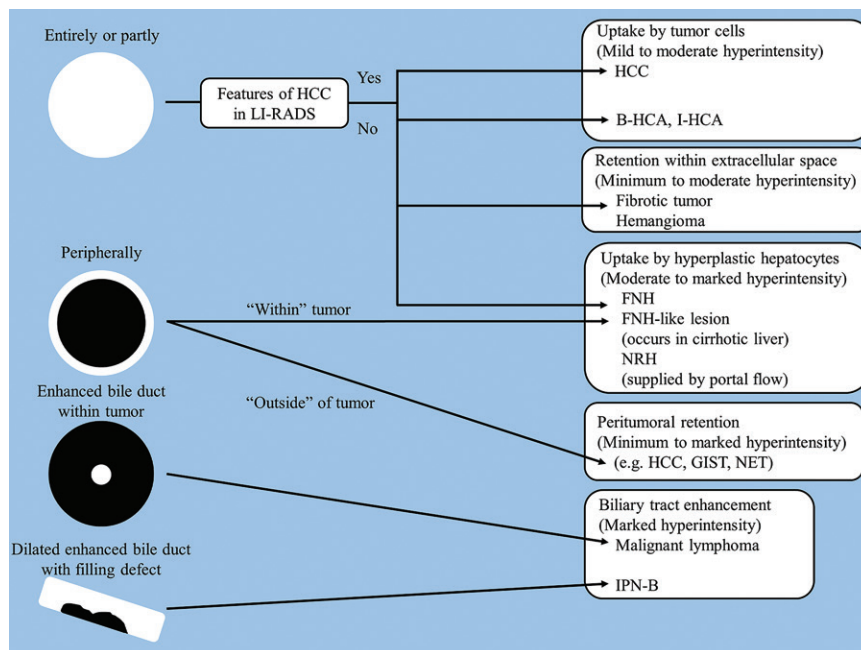


Figure 17. Diagram summarizes the differential diagnosis of hyperintense liver masses seen during the HBP. *GIST* = gastrointestinal stromal tumor, *NET* = neuroendocrine tumor.

recently identified role in the characterization of hepatic masses, including disease and molecular conditions, in addition to its conventional role in facilitating higher detectability of hepatic lesions.

Disclosures of Conflicts of Interest.—*T.N.* Activities related to the present article: disclosed no relevant relationships. Activities not related to the present article: received unrestricted research grants from Bayer AG and Philips Healthcare. Other activities: disclosed no relevant relationships.

References

- Schuhmann-Giampieri G, Schmitt-Willich H, Press WR, Negishi C, Weinmann HJ, Speck U. Preclinical evaluation of Gd-EOB-DTPA as a contrast agent in MR imaging of the hepatobiliary system. *Radiology* 1992;183(1):59–64.
- Bluemke DA, Sahani D, Amendola M, et al. Efficacy and safety of MR imaging with liver-specific contrast agent: U.S. multicenter phase III study. *Radiology* 2005;237(1):89–98.
- Di Martino M, Marin D, Guerrisi A, et al. Intraindividual comparison of gadoxetate disodium-enhanced MR imaging and 64-section multidetector CT in the detection of hepatocellular carcinoma in patients with cirrhosis. *Radiology* 2010;256(3):806–816.
- Yoneda N, Matsui O, Kitao A, et al. Benign Hepatocellular Nodules: Hepatobiliary Phase of Gadoteric Acid-enhanced MR Imaging Based on Molecular Background. *RadioGraphics* 2016;36(7):2010–2027.
- Kierans AS, Kang SK, Rosenkrantz AB. The Diagnostic Performance of Dynamic Contrast-enhanced MR Imaging for Detection of Small Hepatocellular Carcinoma Measuring Up to 2 cm: A Meta-Analysis. *Radiology* 2016;278(1):82–94.
- Motosugi U, Ichikawa T, Morisaka H, et al. Detection of pancreatic carcinoma and liver metastases with gadoteric acid-enhanced MR imaging: comparison with contrast-enhanced multi-detector row CT. *Radiology* 2011;260(2):446–453.
- Quaglia A, Tibballs J, Grasso A, et al. Focal nodular hyperplasia-like areas in cirrhosis. *Histopathology* 2003;42(1):14–21.
- Wanless IR. Micronodular transformation (nodular regenerative hyperplasia) of the liver: a report of 64 cases among 2,500 autopsies and a new classification of benign hepatocellular nodules. *Hepatology* 1990;11(5):787–797.
- Rooks JB, Ory HW, Ishak KG, et al. Epidemiology of hepatocellular adenoma: the role of oral contraceptive use. *JAMA* 1979;242(7):644–648.
- El-Serag HB, Mason AC. Rising incidence of hepatocellular carcinoma in the United States. *N Engl J Med* 1999;340(10):745–750.
- Powers C, Ros PR, Stoupis C, Johnson WK, Segel KH. Primary liver neoplasms: MR imaging with pathologic correlation. *RadioGraphics* 1994;14(3):459–482.
- Cichoz-Lach H, Kasztelan-Szczerbińska B, Słomka M. Gastrointestinal stromal tumors: epidemiology, clinical picture, diagnosis, prognosis and treatment. *Pol Arch Med Wewn* 2008;118(4):216–221.
- Riihimäki M, Hemminki A, Sundquist K, Sundquist J, Hemminki K. The epidemiology of metastases in neuroendocrine tumors. *Int J Cancer* 2016;139(12):2679–2686.
- Huh J. Epidemiologic overview of malignant lymphoma. *Korean J Hematol* 2012;47(2):92–104.
- Lei KI. Primary non-Hodgkin's lymphoma of the liver. *Leuk Lymphoma* 1998;29(3-4):293–299.
- Bronowicki JP, Bineau C, Feugier P, et al. Primary lymphoma of the liver: clinical-pathological features and relationship with HCV infection in French patients. *Hepatology* 2003;37(4):781–787.
- Campos JT, Sirlin CB, Choi JY. Focal hepatic lesions in Gd-EOB-DTPA enhanced MRI: the atlas. *Insights Imaging* 2012;3(5):451–474.
- Chernyak V, Fowler KJ, Kamaya A, et al. Liver Imaging Reporting and Data System (LI-RADS) Version 2018: Imaging of Hepatocellular Carcinoma in At-Risk Patients. *Radiology* 2018;289(3):816–830.
- Goodwin MD, Dobson JE, Sirlin CB, Lim BG, Stella DL. Diagnostic challenges and pitfalls in MR imaging with hepatocyte-specific contrast agents. *RadioGraphics* 2011;31(6):1547–1568.
- Seale MK, Catalano OA, Saini S, Hahn PF, Sahani DV. Hepatobiliary-specific MR contrast agents: role in imaging the liver and biliary tree. *RadioGraphics* 2009;29(6):1725–1748.
- Leonhardt M, Keiser M, Oswald S, et al. Hepatic uptake of the magnetic resonance imaging contrast agent Gd-EOB-DTPA: role of human organic anion transporters. *Drug Metab Dispos* 2010;38(7):1024–1028.

22. König J, Rost D, Cui Y, Keppler D. Characterization of the human multidrug resistance protein isoform MRP3 localized to the basolateral hepatocyte membrane. *Hepatology* 1999;29(4):1156–1163.
23. Kitao A, Matsui O, Yoneda N, et al. The uptake transporter OATP8 expression decreases during multistep hepatocarcinogenesis: correlation with gadoxetic acid enhanced MR imaging. *Eur Radiol* 2011;21(10):2056–2066.
24. Yoneda N, Matsui O, Kitao A, et al. Hepatocyte transporter expression in FNH and FNH-like nodule: correlation with signal intensity on gadoxetic acid enhanced magnetic resonance images. *Jpn J Radiol* 2012;30(6):499–508.
25. Kitao A, Matsui O, Yoneda N, et al. Gadoxetic acid-enhanced magnetic resonance imaging reflects co-activation of β -catenin and hepatocyte nuclear factor 4 α in hepatocellular carcinoma. *Hepatol Res* 2018;48(2):205–216.
26. Kitao A, Matsui O, Yoneda N, et al. Hepatocellular Carcinoma with β -Catenin Mutation: Imaging and Pathologic Characteristics. *Radiology* 2015;275(3):708–717.
27. Elsayes KM, Hooker JC, Agrons MM, et al. 2017 Version of LI-RADS for CT and MR Imaging: An Update. *RadioGraphics* 2017;37(7):1994–2017.
28. Santillan C, Fowler K, Kono Y, Chernyak V. LI-RADS major features: CT, MRI with extracellular agents, and MRI with hepatobiliary agents. *Abdom Radiol (NY)* 2018;43(1):75–81.
29. Tamada T, Ito K, Sone T, et al. Dynamic contrast-enhanced magnetic resonance imaging of abdominal solid organ and major vessel: comparison of enhancement effect between Gd-EOB-DTPA and Gd-DTPA. *J Magn Reson Imaging* 2009;29(3):636–640.
30. Davenport MS, Viglianti BL, Al-Hawary MM, et al. Comparison of acute transient dyspnea after intravenous administration of gadoxetate disodium and gadobenate dimeglumine: effect on arterial phase image quality. *Radiology* 2013;266(2):452–461.
31. Motosugi U, Bannas P, Bookwalter CA, Sano K, Reeder SB. An Investigation of Transient Severe Motion Related to Gadoxetic Acid-enhanced MR Imaging. *Radiology* 2016;279(1):93–102.
32. Motosugi U, Ichikawa T, Sou H, et al. Liver parenchymal enhancement of hepatocyte-phase images in Gd-EOB-DTPA-enhanced MR imaging: which biological markers of the liver function affect the enhancement? *J Magn Reson Imaging* 2009;30(5):1042–1046.
33. Nishie A, Asayama Y, Ishigami K, et al. MR prediction of liver fibrosis using a liver-specific contrast agent: superparamagnetic iron oxide versus Gd-EOB-DTPA. *J Magn Reson Imaging* 2012;36(3):664–671.
34. Wanless IR, Mawdsley C, Adams R. On the pathogenesis of focal nodular hyperplasia of the liver. *Hepatology* 1985;5(6):1194–1200.
35. Hussain SM, Zondervan PE, IJzermans JN, Schalm SW, de Man RA, Krestin GP. Benign versus malignant hepatic nodules: MR imaging findings with pathologic correlation. *RadioGraphics* 2002;22(5):1023–1036; discussion 1037–1039.
36. Prasad SR, Wang H, Rosas H, et al. Fat-containing lesions of the liver: radiologic-pathologic correlation. *RadioGraphics* 2005;25(2):321–331.
37. Suh CH, Kim KW, Kim GY, Shin YM, Kim PN, Park SH. The diagnostic value of Gd-EOB-DTPA-MRI for the diagnosis of focal nodular hyperplasia: a systematic review and meta-analysis. *Eur Radiol* 2015;25(4):950–960.
38. Purysko AS, Remer EM, Coppa CP, Obuchowski NA, Schneider E, Veniero JC. Characteristics and distinguishing features of hepatocellular adenoma and focal nodular hyperplasia on gadoxetate disodium-enhanced MRI. *AJR Am J Roentgenol* 2012;198(1):115–123.
39. Fujiwara H, Sekine S, Onaya H, Shimada K, Mikata R, Arai Y. Ring-like enhancement of focal nodular hyperplasia with hepatobiliary-phase Gd-EOB-DTPA-enhanced magnetic resonance imaging: radiological-pathological correlation. *Jpn J Radiol* 2011;29(10):739–743.
40. Halavaara J, Breuer J, Ayuso C, et al. Liver tumor characterization: comparison between liver-specific gadoxetic acid disodium-enhanced MRI and biphasic CT—a multicenter trial. *J Comput Assist Tomogr* 2006;30(3):345–354.
41. Mohajer K, Frydrychowicz A, Robbins JB, Loeffler AG, Reed TD, Reeder SB. Characterization of hepatic adenoma and focal nodular hyperplasia with gadoxetic acid. *J Magn Reson Imaging* 2012;36(3):686–696.
42. Rebouissou S, Couchy G, Libbrecht L, et al. The β -catenin pathway is activated in focal nodular hyperplasia but not in cirrhotic FNH-like nodules. *J Hepatol* 2008;49(1):61–71.
43. Tang A, Bashir MR, Corwin MT, et al. Evidence Supporting LI-RADS Major Features for CT- and MR Imaging-based Diagnosis of Hepatocellular Carcinoma: A Systematic Review. *Radiology* 2018;286(1):29–48.
44. An C, Rhee H, Han K, et al. Added value of smooth hypointense rim in the hepatobiliary phase of gadoxetic acid-enhanced MRI in identifying tumour capsule and diagnosing hepatocellular carcinoma. *Eur Radiol* 2017;27(6):2610–2618.
45. Narita M, Hatano E, Arizono S, et al. Expression of OATP1B3 determines uptake of Gd-EOB-DTPA in hepatocellular carcinoma. *J Gastroenterol* 2009;44(7):793–798.
46. Kitao A, Zen Y, Matsui O, et al. Hepatocellular carcinoma: signal intensity at gadoxetic acid-enhanced MR Imaging—correlation with molecular transporters and histopathologic features. *Radiology* 2010;256(3):817–826.
47. Cerny M, Chernyak V, Olivie D, et al. LI-RADS Version 2018 Ancillary Features at MRI. *RadioGraphics* 2018;38(7):1973–2001.
48. Palm V, Sheng R, Mayer P, et al. Imaging features of fibrolamellar hepatocellular carcinoma in gadoxetic acid-enhanced MRI. *Cancer Imaging* 2018;18(1):9.
49. McInnes MD, Hibbert RM, Inácio JR, Schieda N. Focal Nodular Hyperplasia and Hepatocellular Adenoma: Accuracy of Gadoxetic Acid-enhanced MR Imaging—A Systematic Review. *Radiology* 2015;277(3):927.
50. Nakashima O, Kurogi M, Yamaguchi R, et al. Unique hypervascular nodules in alcoholic liver cirrhosis: identical to focal nodular hyperplasia-like nodules? *J Hepatol* 2004;41(6):992–998.
51. Calderaro J, Nault JC, Balabaud C, et al. Inflammatory hepatocellular adenomas developed in the setting of chronic liver disease and cirrhosis. *Mod Pathol* 2016;29(1):43–50.
52. Anderson SW, Kruskal JB, Kane RA. Benign hepatic tumors and iatrogenic pseudotumors. *RadioGraphics* 2009;29(1):211–229.
53. Agrawal S, Agarwal S, Arnason T, Saini S, Belghiti J. Management of Hepatocellular Adenoma: Recent Advances. *Clin Gastroenterol Hepatol* 2015;13(7):1221–1230.
54. Zucman-Rossi J, Jeannot E, Nhieu JT, et al. Genotype-phenotype correlation in hepatocellular adenoma: new classification and relationship with HCC. *Hepatology* 2006;43(3):515–524.
55. Bioulac-Sage P, Rebouissou S, Thomas C, et al. Hepatocellular adenoma subtype classification using molecular markers and immunohistochemistry. *Hepatology* 2007;46(3):740–748.
56. Agarwal S, Fuentes-Orrego JM, Arnason T, et al. Inflammatory hepatocellular adenomas can mimic focal nodular hyperplasia on gadoxetic acid-enhanced MRI. *AJR Am J Roentgenol* 2014;203(4):W408–W414.
57. Thomeer MG, EBröker ME, de Lussanet Q, et al. Genotype-phenotype correlations in hepatocellular adenoma: an update of MRI findings. *Diagn Interv Radiol* 2014;20(3):193–199.
58. Thomeer MG, Willemsen FE, Biermann KK, et al. MRI features of inflammatory hepatocellular adenomas on hepatocyte phase imaging with liver-specific contrast agents. *J Magn Reson Imaging* 2014;39(5):1259–1264.
59. Ba-Ssalamah A, Antunes C, Feier D, et al. Morphologic and Molecular Features of Hepatocellular Adenoma with Gadoxetic Acid-enhanced MR Imaging. *Radiology* 2015;277(1):104–113.
60. Tse JR, Naini BV, Lu DS, Raman SS. Qualitative and Quantitative Gadoxetic Acid-enhanced MR Imaging Helps Subtype Hepatocellular Adenomas. *Radiology* 2016;279(1):118–127.
61. Guo Y, Li W, Xie Z, et al. Diagnostic Value of Gd-EOB-DTPA-MRI for Hepatocellular Adenoma: A Meta-Analysis. *J Cancer* 2017;8(7):1301–1310.

62. Glockner JF, Lee CU, Mounajjed T. Inflammatory hepatic adenomas: characterization with hepatobiliary MRI contrast agents. *Magn Reson Imaging* 2018;47:103–110.
63. Sciarra A, Schmidt S, Pellegrinelli A, et al. OATPB1/B3 and MRP3 expression in hepatocellular adenoma predicts Gd-EOB-DTPA uptake and correlates with risk of malignancy. *Liver Int* 2019;39(1):158–167.
64. Bieze M, van den Esschert JW, Nio CY, et al. Diagnostic accuracy of MRI in differentiating hepatocellular adenoma from focal nodular hyperplasia: prospective study of the additional value of gadoxetate disodium. *AJR Am J Roentgenol* 2012;199(1):26–34.
65. Grazioli L, Bondioni MP, Haradome H, et al. Hepatocellular adenoma and focal nodular hyperplasia: value of gadoxetic acid-enhanced MR imaging in differential diagnosis. *Radiology* 2012;262(2):520–529.
66. Yoneda N, Matsui O, Kitao A, et al. Beta-catenin-activated hepatocellular adenoma showing hyperintensity on hepatobiliary-phase gadoxetic-enhanced magnetic resonance imaging and overexpression of OATP8. *Jpn J Radiol* 2012;30(9):777–782.
67. Colletti M, Cicchini C, Conigliaro A, et al. Convergence of Wnt signaling on the HNF4alpha-driven transcription in controlling liver zonation. *Gastroenterology* 2009;137(2):660–672.
68. Fukusato T, Soejima Y, Kondo F, et al. Preserved or enhanced OATP1B3 expression in hepatocellular adenoma subtypes with nuclear accumulation of β -catenin. *Hepatol Res* 2015;45(10):E32–E42.
69. Laumonier H, Bioulac-Sage P, Laurent C, Zucman-Rossi J, Balabaud C, Trillaud H. Hepatocellular adenomas: magnetic resonance imaging features as a function of molecular pathological classification. *Hepatology* 2008;48(3):808–818.
70. van Aalten SM, Thomeer MG, Terkivatan T, et al. Hepatocellular adenomas: correlation of MR imaging findings with pathologic subtype classification. *Radiology* 2011;261(1):172–181.
71. Nault JC, Couchy G, Balabaud C, et al. Molecular Classification of Hepatocellular Adenoma Associates With Risk Factors, Bleeding, and Malignant Transformation. *Gastroenterology* 2017;152(4):880–894.e6.
72. Henriot E, Abou Hammoud A, Dupuy JW, et al. Argininosuccinate synthase 1 (ASS1): a marker of unclassified hepatocellular adenoma and high bleeding risk. *Hepatology* 2017;66(6):2016–2028.
73. Okuda K. Hepatocellular carcinoma: clinicopathological aspects. *J Gastroenterol Hepatol* 1997;12(9-10):S314–S318.
74. Ahn SS, Kim MJ, Lim JS, Hong HS, Chung YE, Choi JY. Added value of gadoxetic acid-enhanced hepatobiliary phase MR imaging in the diagnosis of hepatocellular carcinoma. *Radiology* 2010;255(2):459–466.
75. Golfieri R, Renzulli M, Lucidi V, Corcioni B, Trevisani F, Bolondi L. Contribution of the hepatobiliary phase of Gd-EOB-DTPA-enhanced MRI to dynamic MRI in the detection of hypovascular small (≤ 2 cm) HCC in cirrhosis. *Eur Radiol* 2011;21(6):1233–1242.
76. Nishie A, Asayama Y, Ishigami K, et al. Clinicopathological significance of the peritumoral decreased uptake area of gadolinium ethoxybenzyl diethylenetriamine pentaacetic acid in hepatocellular carcinoma. *J Gastroenterol Hepatol* 2014;29(3):561–567.
77. Choi JW, Lee JM, Kim SJ, et al. Hepatocellular carcinoma: imaging patterns on gadoxetic acid-enhanced MR images and their value as an imaging biomarker. *Radiology* 2013;267(3):776–786.
78. Kitao A, Matsui O, Yoneda N, et al. Hypervascular hepatocellular carcinoma: correlation between biologic features and signal intensity on gadoxetic acid-enhanced MR images. *Radiology* 2012;265(3):780–789.
79. Audard V, Grimmer G, Elie C, et al. Cholestasis is a marker for hepatocellular carcinomas displaying beta-catenin mutations. *J Pathol* 2007;212(3):345–352.
80. Sekine S, Ogawa R, Ojima H, Kanai Y. Expression of SLC01B3 is associated with intratumoral cholestasis and CTNNB1 mutations in hepatocellular carcinoma. *Cancer Sci* 2011;102(9):1742–1747.
81. Mao TL, Chu JS, Jeng YM, Lai PL, Hsu HC. Expression of mutant nuclear beta-catenin correlates with non-invasive hepatocellular carcinoma, absence of portal vein spread, and good prognosis. *J Pathol* 2001;193(1):95–101.
82. Ning BF, Ding J, Yin C, et al. Hepatocyte nuclear factor 4 alpha suppresses the development of hepatocellular carcinoma. *Cancer Res* 2010;70(19):7640–7651.
83. Inoue Y, Yu AM, Yim SH, et al. Regulation of bile acid biosynthesis by hepatocyte nuclear factor 4alpha. *J Lipid Res* 2006;47(1):215–227.
84. Kitao A, Matsui O, Yoneda N, et al. Differentiation Between Hepatocellular Carcinoma Showing Hyperintensity on the Hepatobiliary Phase of Gadoxetic Acid-Enhanced MRI and Focal Nodular Hyperplasia by CT and MRI. *AJR Am J Roentgenol* 2018;211(2):347–357.
85. Joo I, Lee JM, Lee SM, Lee JS, Park JY, Han JK. Diagnostic accuracy of liver imaging reporting and data system (LI-RADS) v2014 for intrahepatic mass-forming cholangiocarcinomas in patients with chronic liver disease on gadoxetic acid-enhanced MRI. *J Magn Reson Imaging* 2016;44(5):1330–1338.
86. Hamm B, Staks T, Mühler A, et al. Phase I clinical evaluation of Gd-EOB-DTPA as a hepatobiliary MR contrast agent: safety, pharmacokinetics, and MR imaging. *Radiology* 1995;195(3):785–792.
87. Yoshikawa J, Matsui O, Kadoya M, Gabata T, Arai K, Takashima T. Delayed enhancement of fibrotic areas in hepatic masses: CT-pathologic correlation. *J Comput Assist Tomogr* 1992;16(2):206–211.
88. Chong YS, Kim YK, Lee MW, et al. Differentiating mass-forming intrahepatic cholangiocarcinoma from atypical hepatocellular carcinoma using gadoxetic acid-enhanced MRI. *Clin Radiol* 2012;67(8):766–773.
89. Min JH, Kim YK, Choi SY, et al. Differentiation between cholangiocarcinoma and hepatocellular carcinoma with target sign on diffusion-weighted imaging and hepatobiliary phase gadoxetic acid-enhanced MR imaging: classification tree analysis applying capsule and septum. *Eur J Radiol* 2017;92:1–10.
90. Ha S, Lee CH, Kim BH, et al. Paradoxical uptake of Gd-EOB-DTPA on the hepatobiliary phase in the evaluation of hepatic metastasis from breast cancer: is the “target sign” a common finding? *Magn Reson Imaging* 2012;30(8):1083–1090.
91. Kim A, Lee CH, Kim BH, et al. Gadoxetic acid-enhanced 3.0T MRI for the evaluation of hepatic metastasis from colorectal cancer: metastasis is not always seen as a “defect” on the hepatobiliary phase. *Eur J Radiol* 2012;81(12):3998–4004.
92. Granata V, Catalano O, Fusco R, et al. The target sign in colorectal liver metastases: an atypical Gd-EOB-DTPA “uptake” on the hepatobiliary phase of MR imaging. *Abdom Imaging* 2015;40(7):2364–2371.
93. Park MJ, Hong N, Han K, et al. Use of Imaging to Predict Complete Response of Colorectal Liver Metastases after Chemotherapy: MR Imaging versus CT Imaging. *Radiology* 2017;284(2):423–431.
94. Park SH, Kim H, Kim EK, et al. Aberrant expression of OATP1B3 in colorectal cancer liver metastases and its clinical implication on gadoxetic acid-enhanced MRI. *Oncotarget* 2017;8(41):71012–71023.
95. Teft WA, Welch S, Lenehan J, et al. OATP1B1 and tumour OATP1B3 modulate exposure, toxicity, and survival after irinotecan-based chemotherapy. *Br J Cancer* 2015;112(5):857–865.
96. Dromain C, Déandréis D, Scoazec JY, et al. Imaging of neuroendocrine tumors of the pancreas. *Diagn Interv Imaging* 2016;97(12):1241–1257.
97. Tamada T, Ito K, Ueki A, et al. Peripheral low intensity sign in hepatic hemangioma: diagnostic pitfall in hepatobiliary phase of Gd-EOB-DTPA-enhanced MRI of the liver. *J Magn Reson Imaging* 2012;35(4):852–858.
98. Doo KW, Lee CH, Choi JW, Lee J, Kim KA, Park CM. “Pseudo washout” sign in high-flow hepatic hemangioma on gadoxetic acid contrast-enhanced MRI mimicking hypervascular tumor. *AJR Am J Roentgenol* 2009;193(6):W490–W496.

99. Yoneda N, Matsui O, Kitao A, et al. Peri-tumoral hyperintensity on hepatobiliary phase of gadoxetic acid-enhanced MRI in hepatocellular carcinomas: correlation with peritumoral hyperplasia and its pathological features. *Abdom Radiol (NY)* 2018;43(8):2103–2112.100.
100. Arnason T, Fleming KE, Wanless IR. Peritumoral hyperplasia of the liver: a response to portal vein invasion by hypervascular neoplasms. *Histopathology* 2013;62(3):458–464.
101. Rocha FG, Lee H, Katabi N, et al. Intraductal papillary neoplasm of the bile duct: a biliary equivalent to intraductal papillary mucinous neoplasm of the pancreas? *Hepatology* 2012;56(4):1352–1360.
102. Lim JH, Yoon KH, Kim SH, et al. Intraductal papillary mucinous tumor of the bile ducts. *RadioGraphics* 2004;24(1):53–66; discussion 66–67.
103. Yeh TS, Tseng JH, Chen TC, et al. Characterization of intrahepatic cholangiocarcinoma of the intraductal growth-type and its precursor lesions. *Hepatology* 2005;42(3):657–664.
104. Oki H, Hayashida Y, Namimoto T, Aoki T, Korogi Y, Yamashita Y. Usefulness of gadolinium-ethoxybenzyl-diethylenetriamine pentaacetic acid-enhanced magnetic resonance cholangiography for detecting mucin retention in bile ducts: a rare intraductal papillary mucinous neoplasm of the bile duct. *Jpn J Radiol* 2011;29(8):590–594.
105. Takanami K, Yamada T, Tsuda M, et al. Intraductal papillary mucinous neoplasm of the bile ducts: multimodality assessment with pathologic correlation. *Abdom Imaging* 2011;36(4):447–456.
106. Ying SH, Teng XD, Wang ZM, et al. Gd-EOB-DTPA-enhanced magnetic resonance imaging for bile duct intraductal papillary mucinous neoplasms. *World J Gastroenterol* 2015;21(25):7824–7833.
107. Yoon HJ, Kim YK, Jang KT, et al. Intraductal papillary neoplasm of the bile ducts: description of MRI and added value of diffusion-weighted MRI. *Abdom Imaging* 2013;38(5):1082–1090.
108. Rajesh S, Bansal K, Sureka B, Patidar Y, Bihari C, Arora A. The imaging conundrum of hepatic lymphoma revisited. *Insights Imaging* 2015;6(6):679–692.
109. Frampas E. Lymphomas: basic points that radiologists should know. *Diagn Interv Imaging* 2013;94(2):131–144.
110. Arora A, Rajesh S, Bihari C. Additional Radiologic Clue to Diagnosing Hepatic Lymphoma. *RadioGraphics* 2015;35(7):2149–2150.

This journal-based SA-CME activity has been approved for AMA PRA Category 1 Credit™. See rsna.org/learning-center-rg.